Geologic Map and Upper Paleozoic Stratigraphy of the Marble Canyon Area, Cottonwood Canyon Quadrangle, Death Valley National Park, Inyo County, California

By Paul Stone, Calvin H. Stevens, Paul Belasky, Isabel P. Montañez, Lauren G. Martin, Bruce R. Wardlaw, Charles A. Sandberg, Elmira Wan, Holly A. Olson, and Susan S. Priest

Pamphlet to accompany

Scientific Investigations Map 3298

2014

U.S. Department of the Interior
U.S. Geological Survey

Cover

View of Marble Canyon area, California, showing dark rocks of Mississippian Indian Springs Formation and Pennsylvanian Bird Spring Formation overlying light rocks of Mississippian Santa Rosa Hills Limestone in middle distance. View is southeast toward Emigrant Wash and Tucki Mountain in distance.

U.S. Department of the Interior
SALLY JEWELL, Secretary

U.S. Geological Survey
Suzette M. Kimball, Acting Director

U.S. Geological Survey, Reston, Virginia: 2014

For more information on the USGS—the Federal source for science about the Earth, its natural and living resources, natural hazards, and the environment—visit *http://www.usgs.gov* or call 1–888–ASK–USGS

For an overview of USGS information products, including maps, imagery, and publications, visit *http://www.usgs.gov/pubprod*

To order this and other USGS information products, visit *http://store.usgs.gov*

Suggested citation:
Stone, P., Stevens, C.H., Belasky, P., Montanez, I.P., Martin, L.G., Wardlaw, B.R., Sandberg, C.A., Wan, E., Olson, H.A., and Priest, S.S., 2014, Geologic map and upper Paleozoic stratigraphy of the Marble Canyon area, Cottonwood Canyon quadrangle, Death Valley National Park, Inyo County, California: U.S. Geological Survey Scientific Investigations Map 3298, scale 1:24,000, 59 p., http://dx.doi.org/10.3133/sim3298.
ISSN 2329–132X (online)

Any use of trade, firm, or product names is for descriptive purposes only and does not imply endorsement by the U.S. Government.

Although this information product, for the most part, is in the public domain, it also may contain copyrighted materials as noted in the text. Permission to reproduce copyrighted items must be secured from the copyright owner.

Contents

Introduction 1
Geologic Framework 2
Upper Paleozoic Stratigraphy and Depositional Environments 4
  Mississippian Rocks 4
  Pennsylvanian and Permian Rocks 8
Late Paleozoic Depositional and Paleogeographic History 17
References Cited 20
Appendix 1—Measured Sections 24
Appendix 2—Mississippian Conodonts, by C.A. Sandberg 39
Appendix 3—Pennsylvanian and Permian Conodonts, by B.R. Wardlaw 42
Appendix 4—Fusulinids and Other Foraminifers, by C.H. Stevens 48
Appendix 5—Corals, by C.H. Stevens 49
Appendix 6—Thin-Section Notes, by C.H. Stevens and P. Stone 51
Appendix 7—Tephrochronologic Analysis of Cenozoic Tuffs, by E. Wan and H.A. Olson 56
Appendix 8—Ammonoids from the Osborne Canyon Formation 5 km East of the Study Area, by P. Stone and C.H. Stevens 59

Figures

1. Index map showing location of geologic map area in Cottonwood Mountains, Death Valley National Park, Inyo County, east-central California 2
2. Chart showing Paleozoic stratigraphy of the Marble Canyon area. 3
3. Field photographs of Upper Mississippian Indian Springs Formation in the Marble Canyon area. 8
4. Field photographs of Pennsylvanian and Permian rocks in the Marble Canyon area 10
5. Maps illustrating Mississippian to Permian paleogeographic evolution of the Inyo Mountains-Cottonwood Mountains area 18
6. Chart showing correlation of members 1–4 of the Bird Spring Formation at Marble Canyon with regional stratigraphic sequences and relative sea-level curve for the Bird Spring Platform 19
7. Thin-section photographs of fusulinids from Pennsylvanian and Permian rocks in the Marble Canyon area 50
8. Thin-section photographs of colonial corals from Pennsylvanian and Permian rocks in the Marble Canyon area 52
9. Photographs of Tertiary tuff outcrops in the map area 58
10. Photographs of ammonoids from the Osborne Canyon Formation 5 km east of the Marble Canyon study area, reproduced from Lee (1975) 59

Geologic Map and Upper Paleozoic Stratigraphy of the Marble Canyon Area, Cottonwood Canyon Quadrangle, Death Valley National Park, Inyo County, California

By Paul Stone[1], Calvin H. Stevens[2], Paul Belasky[3], Isabel P. Montañez[4], Lauren G. Martin[5], Bruce R. Wardlaw[1], Charles A. Sandberg[1], Elmira Wan[1], Holly A. Olson[1], and Susan S. Priest[1]

Introduction

This geologic map and interpretive pamphlet focus primarily on the stratigraphy, depositional history, and paleogeographic significance of upper Paleozoic rocks exposed in the Marble Canyon area in Death Valley National Park, California. The study area, which covers the northwestern part of the Cottonwood Canyon 7.5' quadrangle, is on the east side of the Cottonwood Mountains (northern part of the Panamint Range) about 15 km west of Stovepipe Wells (fig. 1). This area contains excellent exposures of Mississippian to Permian sedimentary rocks that provide important stratigraphic and paleontologic information for reconstructing the late Paleozoic continental margin of the southwestern United States. Vehicular access is provided by a jeep road that starts at Stovepipe Wells and branches into both Marble and Cottonwood Canyons.

Geologic examination of the Marble Canyon area began with mapping studies by Stadler (1968) and Johnson (1971), which established the basic stratigraphic and structural framework. Stone (1984) remapped the area in greater detail with a focus on the Pennsylvanian and Permian rocks. As part of that study, John Repetski of the U.S. Geological Survey identified conodonts that provided the first refined age control for Upper Mississippian to Pennsylvanian rocks exposed in the area. The Mississippian rocks were later studied by Belasky (1988), who included conodont identifications and age determinations by one of the present authors (Sandberg). Most recently, the Pennsylvanian rocks were studied by two of the authors (Martin and Montañez) as part of a regional investigation of sea-level fluctuations on the Bird Spring carbonate platform (Greene, 2010; Martin and others, 2012).

This report synthesizes information from these previous reports together with additional information that has not been presented before. The geologic map is more detailed than that of Stone (1984) and incorporates additional work done from 2009 to 2012. S.S. Priest created the digital database for the geologic map. The measured sections (appendix 1) are from Belasky (1988) and P. Stone (unpublished data, 1980, 1990). We also include updated conodont identifications by C.A. Sandberg and B.R. Wardlaw (appendixes 2 and 3), fusulinid and coral identifications by C.H. Stevens (appendixes 4 and 5), petrographic studies by C.H. Stevens and P. Stone (appendix 6), and a tephrochronologic analysis of Cenozoic tuffs by E. Wan and H.A. Olson (appendix 7). Finally, we include a brief

[1] U.S. Geological Survey.
[2] San Jose State University.
[3] Ohlone College.
[4] University of California, Davis.
[5] Apache Corporation.

discussion of early Permian ammonoids described by Lee (1975) near the mouth of Cottonwood Canyon, 5 km east of the map area (appendix 8).

Mississippian to Permian chronostratigraphic terminology used in this report (fig. 2) is from Davydov and others (2004) and Wardlaw and others (2004). A combination of global and North American stage terms is used as appropriate throughout the report.

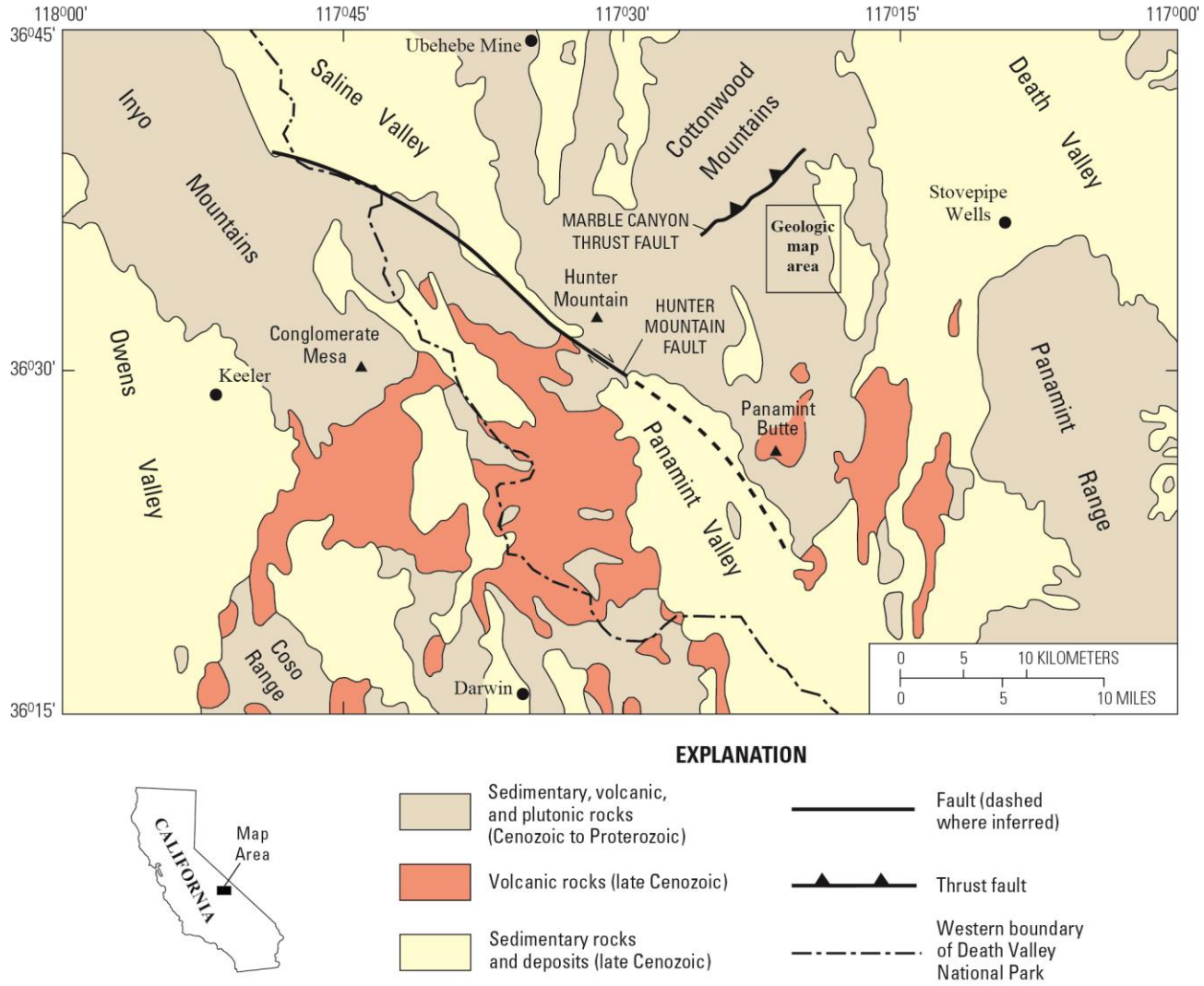

Figure 1. Index map showing location of geologic map area in Cottonwood Mountains, Death Valley National Park, Inyo County, east-central California. Geology generalized from Jennings (1977). Trace of late Cenozoic Hunter Mountain Fault from Burchfiel and others (1987).

Geologic Framework

Bedrock exposed in the Marble Canyon area is composed of Mississippian to lower Permian (Cisuralian) marine sedimentary rocks (fig. 2) and the Jurassic Hunter Mountain Quartz Monzonite. The Mississippian to lower Permian rocks represent lithostratigraphic units that are widespread in east-central California and adjacent regions, although the rocks herein assigned to the Bird Spring Formation are entirely of Pennsylvanian age in contrast to the overall unit age of latest Mississippian to early Permian. Most of the Mississippian to lower Permian rocks are well preserved, but limestone and silty

limestone of the Bird Spring Formation are metamorphosed to marble and calc-silicate rocks near the intrusive contact with quartz monzonite.

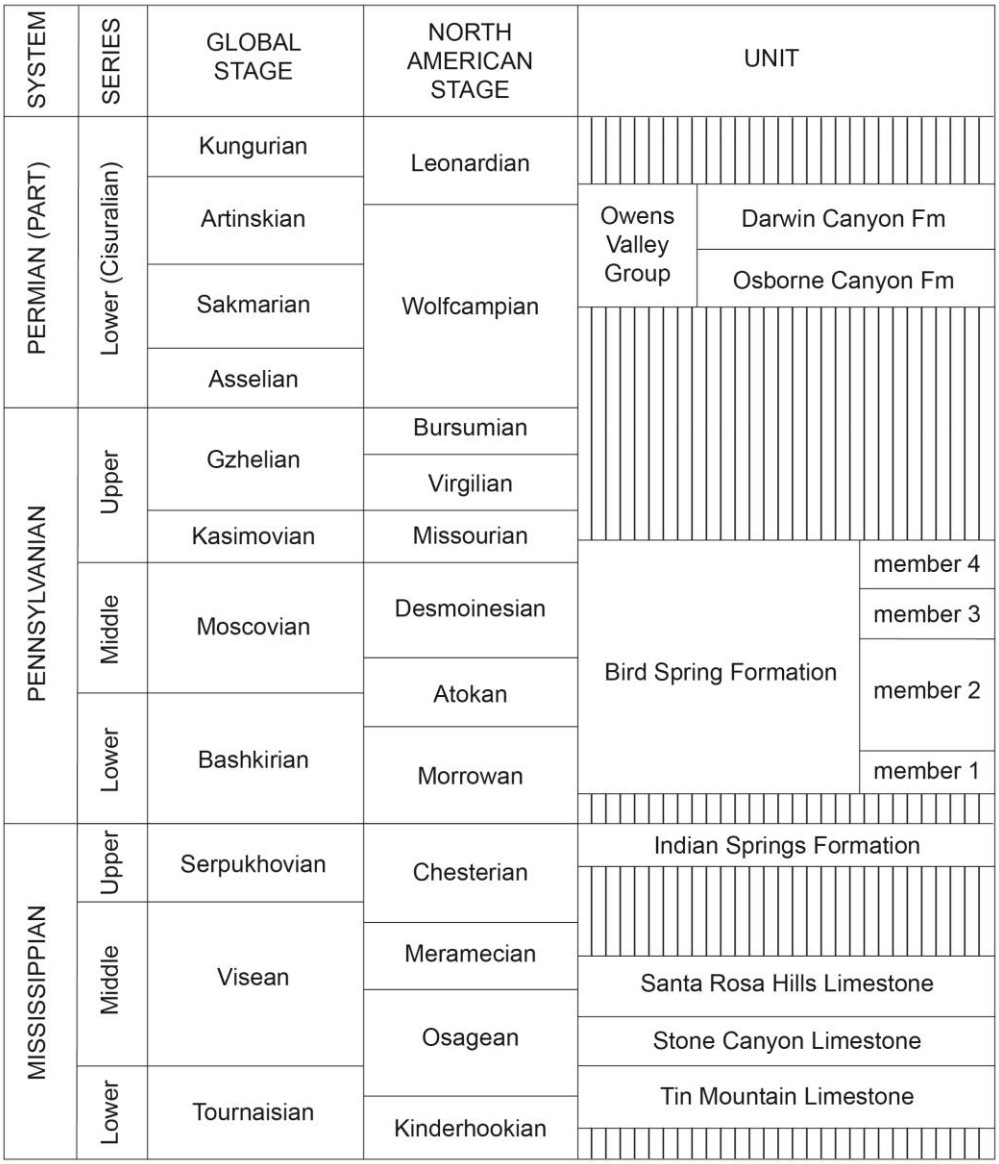

Figure 2. Chart showing Paleozoic stratigraphy of the Marble Canyon area. Stage names and correlations are from Davydov and others (2004) and Wardlaw and others (2004).

The bedrock units are overlain by deeply dissected Tertiary and Quaternary(?) nonmarine sedimentary deposits and minor tuff (unit QTs). The oldest recognized deposits of unit QTs consist of arkosic sandstone and minor conglomerate that we tentatively interpret to represent the middle Miocene Panuga Formation of Snow and Lux (1999). Just east of the map area, however, Snow and Lux (1999) reported older deposits of the lower Miocene Ubehebe Formation, and it is possible that correlative deposits are present in the map area as well. Younger deposits of unit QTs consist primarily of conglomerate that we interpret to represent the middle Miocene to Pliocene Navadu Formation and the Pliocene to Quaternary(?) Nova Formation of Snow and Lux (1999). These younger deposits include a previously unrecognized tuff to which we tentatively assign an age of late middle Miocene (~12 Ma)

based on tephrochronologic analysis, in addition to a tuff dated as ~3.28 Ma and assigned to the Pliocene tuff of Mesquite Spring by Snow and Lux (1999). Both tuffs are further discussed in appendix 7. Younger Quaternary deposits in the map area include moderately dissected alluvium of inferred Pleistocene age (unit Qoa), the alluvium of modern washes (unit Qya), and talus (unit Qt). Unit Qoa contains a slide block of Permian limestone (unit Qsb).

Structurally, the Mississippian to Permian strata are in the lower plate of the Marble Canyon Thrust Fault (Stadler, 1968; Snow, 1992), which is exposed a few kilometers northwest of the map area (fig. 1). This regionally significant thrust fault, which is intruded by the Hunter Mountain batholith beyond the margins of the map area, is interpreted to be of late Permian age (Stevens and Stone, 2005b). Overturned bedding in the lower Permian Osborne Canyon and Darwin Canyon Formations near the west edge of the map area was caused by folding in the lower plate of the thrust fault. Folding, possibly related to intrusion of the Hunter Mountain batholith, deformed Mississippian and Pennsylvanian rocks adjacent to the batholith into a large, northwest-trending anticline that parallels the intrusive contact.

Upper Paleozoic rocks between Marble and Cottonwood Canyons form a series of tilted, northeast-dipping fault blocks bounded by southwest-dipping normal faults (see cross section *A*-*A'*). These faults formed as the result of late Cenozoic extensional deformation of regional extent (Snow and Wernicke, 2000). This faulting and tilting postdated deposition of arkosic sandstone in the lower part of unit QTs, which dips as much as 60° northeast in the hanging wall of a major normal fault and depositionally overlies the Pennsylvanian Bird Spring Formation with little or no angular discordance. Younger deposits of unit QTs dip less steeply and are inferred to have accumulated as the extensional deformation took place. In several places, subhorizontal gravel deposits of unit QTs are bounded by fault scarps, but it is generally unclear whether fault activity predated or postdated deposition of these gravels.

The northwest-striking faults and fault blocks are cut by a major northeast-striking, northwest-dipping normal fault in Marble Canyon. Northeastward along strike, this fault splits into at least two branches that interact with the northwest-striking fault set, resulting in a complex of small fault blocks. Several other northeast-striking, northwest-dipping normal faults are present between Marble and Cottonwood Canyons. In contrast to the major fault in Marble Canyon, however, most of these relatively minor faults appear to be cut by northwest-striking faults.

Upper Paleozoic Stratigraphy and Depositional Environments

The stratigraphic relations and ages of the upper Paleozoic units recognized in the Marble Canyon area are shown in figure 2. The lines of measured sections CC, MC-1, MC-1A, and MC-2, in which the different units are best exposed, are shown on the geologic map. Each measured section is described in detail in appendix 1 and is graphically displayed on the geologic map sheet.

Mississippian Rocks

Rocks of Mississippian age in the Marble Canyon area have an exposed thickness of about 650 m and are composed predominantly of limestone with a thin capping unit of siliciclastic rocks. The thick limestone sequence is divided into three conformable formations that are, in ascending order, the Tin Mountain Limestone, Stone Canyon Limestone (of Stevens and others, 1996), and Santa Rosa Hills Limestone (fig. 2). This sequence of units, widespread in east-central California, is correlative with the lithologically similar Monte Cristo Limestone, or Group, of southern Nevada and southeastern California (Stevens and others, 1996). The Stone Canyon Limestone and Santa Rosa Hills Limestone encompass rocks formerly assigned to the Perdido Formation and Lee Flat Limestone, respectively (Dunne and others, 1981; Stevens and others, 1996). The thin siliciclastic unit that disconformably caps the Mississippian sequence is assigned to the Indian Springs Formation, which is recognized throughout

a large region in eastern California and adjacent parts of Nevada (for example, Stevens and others, 1996).

Tin Mountain Limestone

The Tin Mountain Limestone is recognized only in the vicinity of measured section CC where an incomplete section is exposed and the base is faulted. The depositional contact between the Tin Mountain Limestone and the underlying Devonian Lost Burro Formation is widely exposed in the Cottonwood Mountains outside the map area (Stadler, 1968; Johnson, 1971; Snow, 1990).

The maximum exposed thickness of the Tin Mountain Limestone near section CC is about 100 m, but only the upper 40 m is traversed by the measured section (appendix 1). The rocks consist predominantly of medium-bedded, resistant, dark-gray lime wackestone with thin interbeds of light-red-weathering lime mudstone. The average bed thickness is 20 to 50 cm. Fossils are common and include solitary rugose corals, brachiopods, bryozoans, and siliceous sponge spicules. Pelmatozoan debris occurs throughout and is most abundant near the top of the formation. Chert nodules constitute no more than 10 percent of the rock volume, in contrast to the abundant lenticular chert in the overlying lower member of the Stone Canyon Limestone.

The dark-gray color and fine-grained texture of the Tin Mountain Limestone, together with the abundance of siliceous sponge spicules, suggest deposition on a relatively deep, quiescent carbonate platform (Sandberg and Gutschick, 1984). The presence of stenohaline fossils such as pelmatozoans, bryozoans, and solitary rugose corals implies an offshore environment with good circulation.

Megafossils and conodonts from various localities in east-central California indicate that the Tin Mountain Limestone is of Early Mississippian (Kinderhookian to early Osagean) age (McAllister, 1952, 1956, 1974; Merriam, 1963; Stevens and others, 1996). No fossils were collected or examined from the Tin Mountain Limestone in the study area.

Stone Canyon Limestone

The Stone Canyon Limestone is 417 m thick in measured section CC (appendix 1) where it is informally divided into a lower member (301 m) and an upper member (116 m). The Stone Canyon Limestone conformably overlies the Tin Mountain Limestone and is conformably overlain by the Santa Rosa Hills Limestone.

The lower member of the Stone Canyon Limestone is composed of dark-gray, thin- to medium-bedded lime mudstone, spiculiferous wackestone containing scattered crinoids and rare solitary rugose corals, and about 50 percent black, lenticular chert and brown-weathering, silicified, spiculiferous limestone. The average bed thickness is about 15 cm. The amount of chert and silicified limestone gradually decreases toward the top of the member, while the average bed thickness increases.

The contact with the upper member is marked by the appearance of graded beds of pelmatozoan-rich limestone in addition to the predominant lime mudstone and wackestone like that in the lower member. Graded beds, which commonly exhibit erosive bases, are most abundant in the middle part of the member. Rocks of the upper member are mostly medium gray and contain less chert (30 percent) than rocks of the lower member. Thick, massive beds of medium- to light-gray, coarse-grained pelmatozoan calcarenite are present, although not abundant, in the upper 75 m of the member. Some beds contain colonial tabulate syringoporoid corals and rare, broken colonial rugose corals. Interbeds of lime wackestone locally contain abundant fenestrate bryozoans oriented parallel to bedding.

The contact with the overlying Santa Rosa Hills Limestone is defined by a change in color from medium to light gray, by the disappearance of chert and graded bedding, and by an increase in average bed thickness (from approximately 50 cm to more than 1 m).

The lower member of the Stone Canyon Limestone is interpreted to represent a deep to moderately deep, quiescent, possibly dysaerobic environment of deposition. This interpretation is based on the dark-gray color and generally fine grained texture of the rocks, together with the paucity of megafossils and the abundance of chert (Sando, 1980; Sandberg and Gutschick, 1984; Klingman, 1987). In support of this interpretation, the conodont assemblage in sample PD17 just above the base of the Stone Canyon Limestone represents a gnathodid-pseudopolygnathid biofacies (Lane and others, 1980; Sandberg and Gutschick, 1984), which suggests a foreslope or outer ramp setting.

The upper member of the Stone Canyon Limestone is interpreted to represent a more shallow water depositional environment than the lower member. This interpretation is based on the presence of thick, massive beds of coarse-grained pelmatozoan calcarenite, the local occurrence of colonial rugose corals, and the abundance of graded beds that Belasky (1988) interpreted as storm deposits. Together, these features point to a shallow to moderately shallow water setting with open circulation and varying degrees of water agitation, possibly on a carbonate platform above storm wave base and offshore from high-energy pelmatozoan shoals.

Regionally the Stone Canyon Limestone is late Early to Middle Mississippian (Osagean) in age based primarily on conodonts (Stevens and others, 1996). In the study area (measured section CC), conodonts from sample PD17 just above the base of the formation indicate an early middle Osagean age, whereas conodonts from samples CC-1 and CC-4 approximately 260 and 367 m above the base indicate a middle Osagean age (Stevens and others, 1996; appendix 2). A poorly preserved colonial coral ("*Diphyphyllum*" sp.) from sample PD1, 23 m below the top of the Stone Canyon Limestone, is consistent with a late Osagean age (Belasky, 1988).

Santa Rosa Hills Limestone

The Santa Rosa Hills Limestone is exposed both in Marble Canyon and in Cottonwood Canyon, where it is 109 m thick in measured section CC (appendix 1). The lower part of the formation (37 m thick) is characterized by thick-bedded, light-gray, pelmatozoan packstone and grainstone that contain less than 5 percent nodular chert. The upper part (72 m thick) is of generally similar lithology but also contains several units, up to 10 m thick, composed of medium-gray, predominantly medium-bedded pelmatozoan lime wackestone and as much as 20 percent nodular chert. Locally, rocks in the uppermost 5 m of the formation are medium to dark gray in color. A sharp contact separates the Santa Rosa Hills Limestone from the overlying clastic rocks of the Indian Springs Formation.

The lower part of the Santa Rosa Hills Limestone is interpreted to represent winnowed pelmatozoan shoals deposited in a well-agitated, shallow-water environment. The upper part, which contains substantial amounts of fine-grained limestone and nodular chert, probably represents relatively quiet-water deposition in a partially protected, outer-platform environment.

About 5 km northeast of the map area, near the mouth of Marble Canyon, the upper surface of the Santa Rosa Hills Limestone is marked by circular depressions filled with shale and siltstone that reportedly contain fossils of lycopsid root fragments (*Stigmaria*), *Lepidodendron* cones, and other plant debris (Decourten and Bovee, 1986; locality confirmed by F.L. Decourten, written commun., 2012). The presence of these fossils led Decourten and Bovee (1986) to interpret the depressions as "an exhumed rooting ground representing a buried forested shoal." Bishop and others (2009) reported similar potholes and *Stigmaria* at the top of the Mississippian limestone sequence at Arrow Canyon, Nevada, 250 km east of Marble Canyon.

Regionally the Santa Rosa Hills Limestone is Middle Mississippian (late Osagean to early Meramecian) in age based primarily on conodonts (Stevens and others, 1996). In the study area, conodonts from sample CC-6, 16 m above the base of the formation in measured section CC, indicate a

late Osagean age, and conodonts from the upper meter of the formation in measured section MC-1 (samples MC-1-1, 90-MC-1) indicate an early Meramecian age (Stevens and others, 1996; appendix 2).

Indian Springs Formation

Rocks assigned to the Indian Springs Formation consist of sandstone, shale, and minor limestone that form a generally red-weathering recessive interval between the more resistant limestone units above and below. This formation, which commonly is partially or completely covered by talus or colluvium, is between 15 and 20 m thick throughout the study area.

Some of the best exposures of the Indian Springs Formation are in the vicinity of measured section MC-1A (appendix 1) where it is about 18 m thick. There, the lower 11 m of the formation are mostly composed of greenish-gray, ochre, and reddish-brown shale interspersed with beds of clastic limestone. A conspicuous bed of clastic limestone, a brachiopod-fragment coquina 0.7 m thick, is present 2 m above the base of the formation (fig. 3*A*). This laterally continuous bed was recognized at several other localities in the map area, including measured section MC-1 (appendix 1). Petrographic examination shows that this bed contains a variety of clasts in addition to brachiopod fragments, including crinoid ossicles, bryozoans, echinoid spines, and phosphatic fragments, some of which are phosphatized fossil fragments (appendix 6, sample MC-1-2).

The overlying 6 m of strata in measured section MC-1A are composed primarily of resistant, ledge-forming calcareous sandstone that mostly weathers rusty brown. The sandstone is fine to medium grained and displays well-developed planar and cross lamination (fig. 3*B*). Petrographic thin sections of several sandstone samples reveal that the rocks are quartzose, mostly well sorted, and cemented with calcite; some samples contain reworked foraminifers and shell fragments (appendix 6). At the top of this sequence is a 0.3-m-thick bed of sandy to conglomeratic limestone that contains dark-brown phosphatic clasts as much as 2 cm in diameter (fig. 3*C*). On the upper surface of this bed about 0.2 km west of measured section MC-1A, we observed a fossil (fig. 3*D*) that has been tentatively identified as a ctenacanth shark spine (Eileen Grogan, Bill DiMichele, and Hermann Pfefferkorn, written and oral commun., 2010).

The uppermost rocks that we assign to the Indian Springs Formation, covered or poorly exposed at most localities, are unusually well exposed in a stream cut near measured section MC-1A. There, the sandy to conglomeratic limestone bed is overlain by 1.4 m of pink to gray, fissile, calcareous siltstone and fine-grained sandstone, parts of which contain phosphatic grains, abraded brachiopods, burrows, and possible plant fossils. These relatively recessive rocks are sharply overlain by more resistant silty limestone that we map as the basal part of the Bird Spring Formation.

The abundance of pervasively laminated and cross-laminated, well-sorted sandstone in the Indian Springs Formation, particularly in the upper part, suggests a shallow-water, near-shore, high-energy depositional environment conducive to the reworking of bioclastic material. The lower, shale-rich part of the formation probably represents deposition in somewhat quieter and perhaps deeper water. The coquina near the base of the formation could represent a storm deposit.

Regionally the Indian Springs Formation is considered to be of Late Mississippian (late Chesterian) age based on megafossils and conodonts (Stevens and others, 1996). In the map area, sample MC-1-2 from the coquina 1.5 m above the base of the Indian Springs Formation contains conodonts indicating an early Chesterian age (appendix 2). It is uncertain if this age represents the time of deposition or if the conodonts were reworked from older rocks. In either case, these conodonts demonstrate that the contact with the underlying Santa Rosa Hills Limestone represents a hiatus at least spanning most of Meramecian time. Fragmentary conodonts from sample MC-1A-5 near the top of the Indian Springs Formation suggest a late Chesterian age, but the fauna is not well enough preserved to support a definitive age assignment.

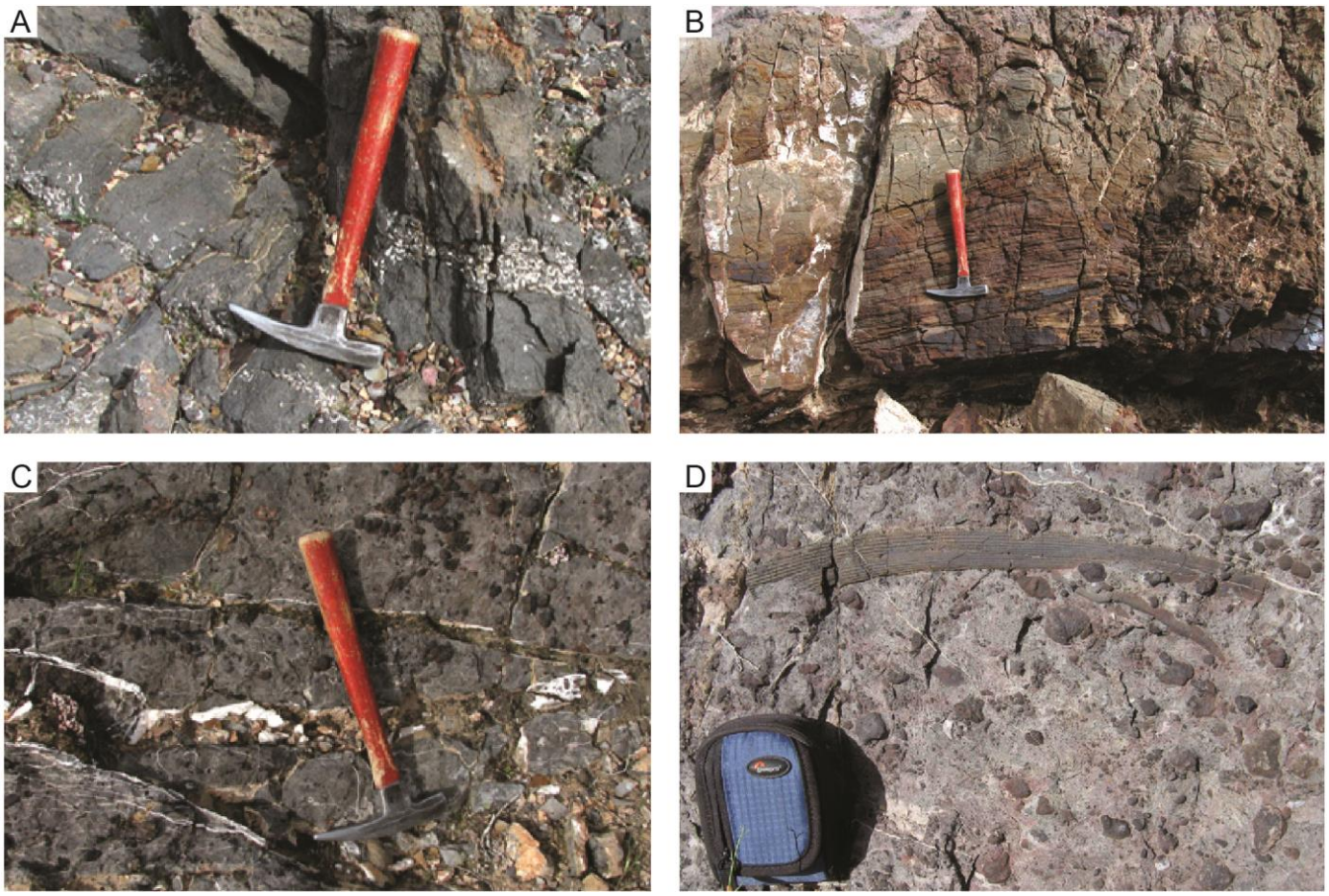

Figure 3. Field photographs of Upper Mississippian Indian Springs Formation in the Marble Canyon area. *A*, Coquina with small white shell fragments about 2 m above base of formation (measured section MC-1A, unit 3). *B*, Cross-laminated sandy calcarenite near top of formation, near measured section MC-1A. *C*, Dark phosphatic nodules on upper surface of sandy to conglomeratic limestone bed near top of formation, near measured section MC-1A. *D*, Fossil tentatively identified as a ctenacanth shark spine on same bedding surface shown in *C*.

Pennsylvanian and Permian Rocks

Rocks of Pennsylvanian and Permian age, which have a maximum thickness of about 1,150 m, crop out extensively in the Marble Canyon area. In ascending order, these rocks are assigned to the Bird Spring, Osborne Canyon, and Darwin Canyon Formations, the latter two of which comprise the Owens Valley Group (fig. 2). These unit assignments are based on lithostratigraphic correlations with the type section of the Bird Spring Formation in southern Nevada (Hewett, 1931) and the type sections of the Osborne Canyon and Darwin Canyon Formations in the vicinity of Darwin, California (Stone and others, 1987), some 40 km southwest of the Marble Canyon area (fig. 1).

Rocks herein assigned to the Bird Spring Formation were originally mapped as the Keeler Canyon Formation (Stadler, 1968; Johnson, 1971), the type area of which is in the Inyo Mountains about 40 km west of Marble Canyon (fig. 1). Subsequent studies (Stone, 1984; Stone and Stevens, 1984) showed that the Keeler Canyon Formation consists largely of deep-water turbidites that do not closely resemble most of the rocks previously assigned to that formation at Marble Canyon, and that these rocks are more appropriately assigned to the Bird Spring Formation, which consists primarily of shelf deposits (Stevens and Stone, 2007). Prior to definition of the Osborne Canyon and Darwin Canyon Formations as

part of the Owens Valley Group, rocks herein assigned to these units at Marble Canyon were mapped as the Owens Valley Formation (Stadler, 1968; Johnson, 1971).

Bird Spring Formation

The Bird Spring Formation is about 600 m thick in the eastern part of the study area but thins to about 425 m in the southwestern part. The formation is composed primarily of thin-bedded, variably cherty and silty limestone, but it also includes a distinctive basal sequence of relatively thick bedded silty limestone and a sequence of thick-bedded to massive, fossiliferous limestone near the top. In addition, the sequence contains several intervals of slumped and contorted limestone and marly limestone that grade laterally into monomictic breccia and are intercalated with polymictic breccia (Greene, 2010; Martin and others, 2012). In the eastern part of the map area, where the rocks are essentially unmetamorphosed, the Bird Spring Formation typically forms steep, ledgy slopes of alternating gray- and grayish-yellow-weathering beds. By contrast, in the western part of the area near the Hunter Mountain Quartz Monzonite, the rocks are metamorphosed to dark-brown-weathering calc-hornfels and gray marble.

Lithology

In the area of measured section MC-1, where it is thickest and best exposed, the Bird Spring Formation is divided into four informal members. Member 1, which constitutes the lower 38 m of the Bird Spring Formation in measured section MC-1 and the lower 43 m in measured section MC-1A, consists of buff-weathering, fine-grained, silty limestone that forms resistant, planar beds 0.5 to 3 m thick (fig. 4*A*). Most limestone beds are calcisiltite composed of well-sorted, silt-size micritic peloids, subangular detrital quartz, and subordinate abraded bioclasts and sponge spicules (appendix 6, sample MC-1-4). Some beds are normally graded and are weakly cross laminated, contain mudstone rip-up clasts and granule- to pebble-size lithoclasts at the base, and grade upward into massive or plane-laminated, fine-grained limestone. The resistant beds of silty limestone are separated by recessive layers of buff to pinkish-gray silty limestone or calcareous siltstone 3 to 15 cm thick. Lenses and layers of dark-brown chert 3 to 10 cm thick are common, particularly near the tops of the resistant silty limestone beds. These features combine to produce an overall appearance of very even, tabular stratification. Member 1 is capped by a 0.5-m-thick unit of contorted limestone beds (basal unit of member 2; fig. 4*B*) that show soft-sediment deformation and grade laterally into monomicitic breccia of clast composition similar to the adjacent undeformed limestone (Greene, 2010; Martin and others, 2012).

Member 2, which is 379 m thick in measured section MC-1 and forms the bulk of the Bird Spring Formation, is primarily composed of very fine grained limestone containing abundant nodular and lenticular chert (fig. 4*C*). Most of the limestone is light to medium gray or buff in color, but dark-gray and pinkish- to purplish-gray limestone also is common. Petrographic examination of several samples (appendix 6) shows that the limestone is generally micrite or calcisiltite containing as much as 40 percent detrital quartz. Sponge spicules, radiolarians, and ostracodes are also present in some samples. Typically the limestone forms planar, unlaminated to finely laminated or graded beds of alternating color 5 to 50 cm thick (fig. 4*D*); slumped and contorted limestone beds and associated monomictic breccia are rare. Within and between many limestone beds are lenses and aligned nodules of dark-brown to black chert that further enhance the stratification. Exposed bedding surfaces commonly display abundant chert nodules. Spherical (“golf ball”) chert nodules that average about 2 cm in diameter are particularly abundant, but elongate to irregular nodules of diverse size and shape are common as well.

Macrofossils, primarily crinoidal debris and bryozoans, are rare in the lower 310 m of member 2 but are more common above that level, where gastropods and articulated crinoid stems also are present

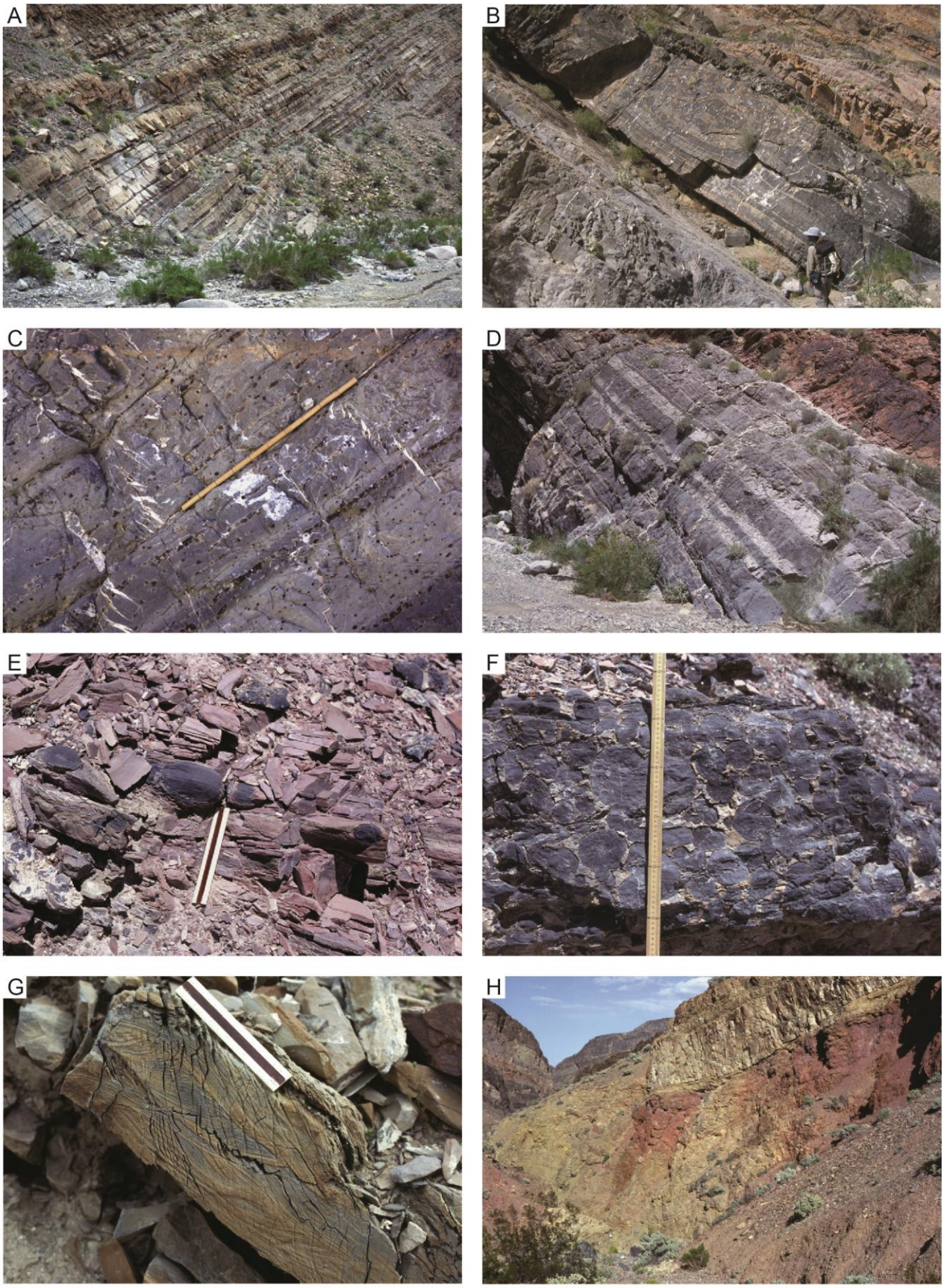
A
B
C
D
E
F
G
H

Figure 4. (Previous page) Field photographs of Pennsylvanian and Permian rocks in the Marble Canyon area. *A*, Bird Spring Formation, member 1, silty limestone forming resistant, planar beds interpreted as turbidites (measured section MC-1, unit 5). *B*, Bird Spring Formation, contorted limestone beds at base of member 2 (measured section MC-1, unit 7). *C*, *D*, Bird Spring Formation, member 2, micritic limestone forming alternating light-gray and medium-gray beds containing lenses and nodules of chert (measured section MC-1, unit 58). *E*, Osborne Canyon Formation, member 3, pink silty mudstone containing dark-gray spherical limestone concretions (measured section MC-2, unit 19). *F*, Osborne Canyon Formation, member 3, conglomerate consisting of tightly packed, spherical limestone clasts that probably are redeposited concretions (measured section 2, unit 20). *G*, Darwin Canyon Formation, cross-laminated calcareous siltstone to very fine grained sandstone (measured section 2, unit 63). *H*, Darwin Canyon Formation, massive bed of red-weathering, very fine grained silty limestone containing unsorted, matrix-supported limestone clasts and bioclasts that include fusulinids and coral fragments, interpreted as a debris-flow deposit; sharply overlain by siltstone to very fine grained sandstone (fossil locality 80-MC-1; see geologic map).

locally. Skeletal wackestone, packstone, and grainstone typify the upper 60 m of member 2. For example, thin-section sample MC-1-33, about 317 m above the base of member 2, is a grainstone containing small fusulinids and brachiopod shell fragments (appendix 6). Chert is relatively uncommon in beds containing abundant fossil debris.

Member 3, 76 m thick in measured section MC-1, is characterized by the presence of thick-bedded to massive, medium- to dark-gray, skeletal limestone that forms most of the lower 33 m of the member and isolated beds 4 to 6 m thick in the upper 43 m. The skeletal limestone is mostly coarse-grained packstone, grainstone, and minor wackestone. Heterozoan skeletal limestone beds contain crinoid columnals, echinoid spines, encrusting and fenestrate bryozoans, brachiopods, sponges, trilobites, and palaeotextulariid foraminifers. Fusulinids are present in skeletal limestone beds along with algal-coated skeletal fragments (for example, appendix 6, sample MC-1-41). A colonial coral (*Petalaxis yosti* Stevens, 1995; appendix 5) was found on the upper surface of a skeletal packstone bed at the top of member 3.

Micritic limestone in various shades of gray, buff, and pinkish gray forms most of the upper 43 m of member 3. This limestone contains abundant lenses and aligned nodules of brown to black chert that typically form planar zones 5 to 10 cm thick. These rocks resemble those of member 2 but are less distinctly bedded. Decimeter-scale lenses of grainstone and packstone that fill scours within the micritic limestone consist of abundant broken or abraded skeletal grains, commonly with micritic coatings. A polymictic breccia containing abraded pebble- to boulder-size clasts of calcisiltite and bioclastic limestone is locally present near the top of member 3.

Member 4, which constitutes the upper 108 m of the Bird Spring Formation in measured section MC-1, consists primarily of interlayered buff and light- to medium-gray micritic limestone (including calcisiltite, wackestone, and packstone) that produce a distinctive color-banded appearance. Beds range from 15 cm to 1 m thick. The buff limestone beds typically contain abundant nodules, lenses, and thin (5 to 15 cm) beds of brown chert that enhance the stratification. The gray limestone beds generally lack chert but commonly are bounded above and below by cherty layers. In contrast to the dominant small, spherical nodules of member 2, chert nodules in member 4 are generally larger and more irregular in shape. Thin, planar to lenticular concentrations of fossil debris, mostly crinoidal, are present in the micritic limestone beds, particularly in the lower 20 m of the member. Also present in member 4 are a few isolated, ledge-forming beds of medium- to dark-gray skeletal (crinoid-dominated) limestone (packstone and wackestone) 5 to 7.5 m thick. The lowest such bed, which contains small solitary rugose corals, pinches out laterally within 50 m in both directions from the line of measured section MC-1.

Depositional Environments

The predominance of silty, fine-grained limestone and the presence of interbedded contorted and slumped carbonate beds and breccias indicate an outer-platform to upper-slope environment for most of the Bird Spring Formation at Marble Canyon. The tabular, graded, silty limestone beds of member 1, which we interpret as turbidites, indicate a deep-water environment below storm wave base at the onset of Bird Spring deposition. Slumped limestone beds exhibiting soft-sediment deformation just above the top of member 1 are interpreted to have formed in a slope environment.

Micritic limestone and calcisiltite of member 2 are interpreted to have accumulated in an outer-platform to upper-slope environment. Storm-induced currents transported silt-sized sediment, bioclasts and detrital quartz to these environments from the inner and middle platform. Fossiliferous packstone and grainstone toward the top of member 2 are interpreted to have formed in skeletal banks between storm and fair-weather wave base. Diverse fauna and common bioturbation suggest normal-marine conditions. These fossiliferous beds suggest the seaward progradation of mid-platform carbonates to the outer platform.

Member 3 is characterized by the abundance of fossiliferous wackestone, packstone, and grainstone. The presence of abundant broken or abraded skeletal grains and the intercalation of mud-rich skeletal limestone with decimeter-scale lenses of grainstone and packstone filling scours indicate that these bioclastic limestones were transported from skeletal banks inboard of Marble Canyon. The overall predominance of grainy skeletal limestone in the lower half of member 3 strongly suggests seaward progradation of the platform during extended periods of member 3 deposition.

The predominantly fine-grained limestone of member 4 is interpreted to record a return to a deeper-water, outer-platform depositional environment similar to that of member 2. Isolated bioclastic limestone beds presumably derived from inboard skeletal banks are present in the lower part of member 4 but decrease in abundance upward through the section, reflecting progressive deepening of the platform and increasing distance from the shallow-water banks.

Fossils and Age

Age-diagnostic fossils recovered from the Bird Spring Formation in the Marble Canyon area include both conodonts and fusulinids. All of the fossils are from measured section MC-1 except one conodont sample from measured section MC-2. Conodonts were recovered from numerous horizons in the formation, whereas identifiable fusulinids are largely restricted to member 3.

Conodonts from the Bird Spring Formation in measured section MC-1 indicate an age range of Bashkirian to Kasimovian (Morrowan to Missourian). The age determinations presented here (appendix 2) generally support the original age determinations by John Repetski (*in* Stone, 1984).

Conodonts indicating a Bashkirian age extend from the lowest sample 1.5 m above the base of member 1 (MC-1-4) to sample MC-1-18, about 132 m above the base of the formation and 94 m above the base of member 2. Faunas of earliest Bashkirian (early Morrowan) age are not represented. Above MC-1-18 is a barren interval that extends to sample MC-1-25, about 258 m above the base of the formation and 220 m above the base of member 2. Conodonts indicating a Moscovian age first appear in sample MC-1-25 and extend through sample MC-1-51, 538 m above the base of the Bird Spring Formation and 45 m above the base of member 4. Thus, the upper part of member 2, member 3, and the lower part of member 4 are all Moscovian based on the conodont assemblages. The stratigraphically highest conodonts in member 4, from two samples (MC-1-52, 53) in the upper 63 m of measured section MC-1 and from sample MC-2-1 about 13 m below the top of the Bird Spring Formation in measured section 2, indicate a Kasimovian (Missourian) age. Lithostratigraphic correlation between measured sections MC-1 and MC-2 indicates that sample MC-2-1 is probably only a meter or two higher than sample MC-1-51, the highest sample interpreted as Moscovian.

Identifiable fusulinids were recovered from two localities in member 3 of the Bird Spring Formation in measured section MC-1 (appendix 4, samples S-1507, -1508, -2100). These fusulinids indicate a Desmoinesian age, compatible with the associated Moscovian conodonts.

Erosional Contact with Osborne Canyon Formation

The upper part of measured section MC-1 (on the east side of the Marble Canyon wash) does not extend to the contact between member 4 of the Bird Spring Formation and the overlying Osborne Canyon Formation (see geologic map). This contact, however, is exposed in a steep gulch on the west side of the Marble Canyon wash. There, massive conglomeratic mudstone at the base of the Osborne Canyon Formation overlies well-bedded silty limestone of member 4 similar to that in the upper part of measured section MC-1. Followed westward up this gulch, the base of the Osborne Canyon Formation cuts downward through member 4 at a low angle, indicating that the contact is erosional.

The contact between the Bird Spring and Osborne Canyon Formations also is exposed in measured section 2. Detailed lithostratigraphic correlation indicates that the 65 m of Bird Spring strata in measured section 2 correspond to the lower 57 m of member 4 in measured section 1 (see stratigraphic column on map sheet). Thus, the upper 51 m of member 4 in measured section 1 are not represented in measured section 2, providing further indication that the lower contact of the Osborne Canyon Formation is erosional.

Direct evidence of erosion along the Bird Spring-Osborne Canyon contact is found in the vicinity of measured section 2, where we have observed that the basal Osborne Canyon Formation cuts downward through the Bird Spring Formation at a low angle from southeast to northwest along strike. Traced 1 km northwest from measured section MC-2, all 65 m of Bird Spring strata measured in section MC-2 are progressively cut out beneath the contact, with a corresponding increase in the thickness of the basal part of the Osborne Canyon Formation. This relation suggests that the contact represents part of a channel that was eroded into the Bird Spring Formation prior to deposition of the Osborne Canyon Formation.

Osborne Canyon Formation

The Osborne Canyon Formation, which averages about 150 m thick in the map area, disconformably overlies the Bird Spring Formation and is conformably overlain by the Darwin Canyon Formation. The Osborne Canyon Formation is composed of silty calcareous mudstone, very fine grained calcareous sandstone, siliceous mudstone or chert, conglomeratic limestone, and minor calcarenitic limestone. The fine-grained rocks, which dominate the lower half of the formation, form recessive, generally pink or purple slopes, whereas the more resistant conglomeratic and calcarenitic limestone beds form dark-gray ledges that characterize the upper half of the formation. Viewed from a distance, the Osborne Canyon Formation typically forms a distinctive, purplish-gray to dark-gray band between the lighter gray Bird Spring Formation below and the brown Darwin Canyon Formation above. The Osborne Canyon Formation is thickest in areas where the disconformable lower contact cuts deepest into the underlying Bird Spring Formation.

In measured section MC-2, where the Osborne Canyon Formation is 150 m thick, it is divided into four informal members. Member 1, comprising the lower 36 m of the formation, is primarily composed of silty calcareous mudstone that varies in color from purplish- or pinkish-gray to greenish-gray and buff. This mudstone is interbedded with medium-gray, fine-grained, plane-laminated to cross-laminated calcareous sandstone that forms discrete beds 2 to 20 cm thick with sharp bases and tops. Petrographic examination shows that both the mudstone and sandstone contain bioclastic material including crinoid fragments, possible algal fragments, and small foraminifers (appendix 6, samples MC-2-3A–D). Lenses of dark-gray micritic limestone are present but rare.

Member 2, 43 m thick, consists of thinly interbedded, pink to purple, silty mudstone and black chert. The mudstone contains abundant limestone concretions that are 2 to 15 cm in diameter and range in shape from spherical to flattened in the plane of bedding (fig. 4*E*). Some beds consist almost entirely of limestone concretions. The interbedded chert contains abundant radiolarians as seen in thin section (appendix 6, sample MC-2-5).

Member 3, 47 m thick, is characterized by limestone conglomerate that forms discrete beds about 0.2 to 3 m thick. This lithologically distinct conglomerate is composed of tightly packed, poorly sorted, mostly spherical clasts of limestone (probably redeposited concretions) ranging from 1 to 15 cm in diameter (fig. 4*F*). Conglomerate beds are interlayered with limestone-concretion-bearing, silty mudstone and black chert similar to the rocks of member 2. Petrographic examination of a limestone concretion extracted from mudstone reveals scattered ostracodes, peloids, chert(?) fragments, and possible radiolarians (appendix 6, sample MC-2-10).

Member 4, which constitutes the upper 24 m of the Osborne Canyon Formation, is distinguished by the presence of dark-gray, coarse-grained, calcarenitic and bioclastic limestone that forms discrete beds 0.3 to 0.7 m thick. Member 4 also is distinguished by the presence of two closely spaced beds of massive, purplish-red, silty mudstone that contains spherical limestone concretions and ammonoids. Some ammonoids are free and some are enclosed in limestone concretions. Apart from these distinctive rock types, member 4 is similar to member 3, mainly consisting of light-gray, pinkish-gray, and buff, silty calcareous mudstone with sparse spherical limestone concretions, scattered beds of limestone conglomerate 0.2 to 0.3 m thick, and minor thin-bedded chert.

Rocks of the Osborne Canyon Formation in the map area differ from those in the type section of the formation near Darwin, where the formation lacks limestone conglomerate with spherical limestone clasts and contains abundant graded beds of fusulinid-bearing bioclastic limestone (Stone and others, 1987). Only 4 km east of the type section, however, the Osborne Canyon Formation closely resembles the section in the Marble Canyon area, with a lower half composed of calcareous mudstone containing spherical limestone concretions and an upper half composed of limestone conglomerate with spherical limestone clasts (Stone, 1984, p. 89-90). This similarity supports our assignment of the rocks at Marble Canyon to the Osborne Canyon Formation.

The predominance of laminated mudstone and radiolarian chert in the Osborne Canyon Formation, together with the absence of sedimentary features or fossils suggesting deposition in shallow water, points to a relatively deep water depositional environment. We suggest that deposition took place in a slope setting where limestone concretions formed in place during or shortly after deposition of the enclosing laminated mudstone. The associated conglomerates, which contain little or no bioclastic material, probably represent sediment-gravity-flow deposits formed primarily of reworked limestone concretions derived from higher on the slope. By contrast, the bioclastic calcarenites of member 4 probably were derived from a shallow-water shelf. Graded bioclastic limestone beds in the type section of the Osborne Canyon Formation near Darwin clearly were deposited as deep-water turbidites derived from a carbonate shelf (Stone, 1984; Stone and others, 1987).

Age control on the Osborne Canyon Formation in the Marble Canyon study area is limited to conodont samples MC-2-10, -11, and -14 from members 3 and 4 in measured section MC-2 (appendix 3). Conodonts from these samples indicate an early Permian (probably basal Artinskian) age. Of several samples collected for conodonts from underlying rocks in the Osborne Canyon Formation, only reworked fragments of middle Pennsylvanian conodonts were found in the lone productive sample (MC-2-4 from a limestone lens in member 1). Ammonoids from the lower 15 m of the Osborne Canyon Formation about 5 km east of the study area indicate an early Permian (Sakmarian) age (Lee, 1975; see appendix 8).

Darwin Canyon Formation

The Darwin Canyon Formation in the Marble Canyon area is about 400 m thick with the depositional top not exposed because of faulting and erosion. The formation is composed primarily of brown-weathering, calcareous siltstone to very fine grained sandstone that contrasts sharply with the predominant pink to purple mudstone of the underlying Osborne Canyon Formation. Minor calcarenitic limestone, conglomerate, and rare chert also are present.

The siltstone to very fine grained sandstone that dominates the Darwin Canyon Formation typically is pervasively plane- to cross-laminated (fig. 4*G*) and stands out in thick ledges that alternate with more recessive intervals. From a distance the formation appears thick and evenly bedded, but individual beds can be difficult to distinguish when viewed from closer range. Fresh rock surfaces vary in color from pale red to light reddish gray and pale gray. Petrographic examination of several samples from measured section MC-2 (appendix 6) shows 30 to 70 percent well sorted quartz silt to very fine sand (average grain diameter about 0.075 mm) and most of the remainder calcite, some of which is undoubtedly of detrital origin. Minor detrital feldspar and muscovite are also present. Crinoid fragments, foraminifers, and other bioclasts are present in some thin sections. Locally, the siltstone to very fine grained sandstone alternates with recessive intervals of thin-bedded mudstone, siltstone, and radiolarian chert (for example, measured section MC-2, unit 75).

Scattered in the Darwin Canyon Formation are isolated beds of dark-gray, medium- to coarse-grained calcarenitic limestone and limestone conglomerate that range from less than a meter to about 2 m thick. Field and petrographic examination shows that these beds contain a variety of bioclasts including fragments of crinoids, brachiopods, bryozoans, algae, fusulinids, and other foraminifers (appendix 6). Limestone intraclasts are also present. The bioclasts and intraclasts typically are embedded in a matrix of calcareous sandstone. The coarsest limestone beds are massive, but some coarse- to medium-grained beds are plane- to cross-laminated. One graded bed was observed (measured section MC-2, unit 68).

Near the top of the Darwin Canyon Formation is a massive bed of orange- to red-weathering, very fine grained silty limestone containing unsorted, matrix-supported limestone clasts and bioclasts that include fusulinids and coral fragments. This bed is best exposed about 1 km south of measured section MC-2 (fossil localities 80-MC-1 and SJS-1087; see geologic map), where it is about 20 m thick and is sharply overlain and underlain by bedded siltstone to very fine grained sandstone (fig. 4*H*). The basal part of this bed contains large clasts of medium- to dark-gray limestone in which ammonoids are locally abundant. The same or a very similar bed is exposed near the top of the Darwin Canyon Formation 0.5 km north of measured section MC-2 (fossil localities 80-MC-3 and S-1487), although this bed was not encountered in the measured section itself.

The siltstone to very fine grained sandstone that composes the bulk of the Darwin Canyon Formation in the Marble Canyon area is lithologically very similar to that which typifies the type section of the Millers Spring Member of the Darwin Canyon Formation near Darwin (Stone and others, 1987). In addition, the massive, silty limestone bed near the top of the section in the Marble Canyon area bears a striking resemblance to a bed of similar lithology, color, and thickness in the Millers Spring Member near Darwin. Finally, the isolated limestone beds in the Darwin Canyon Formation at Marble Canyon are lithologically similar to limestone beds in the type section of the Millers Spring Member, although they do not form thick, mappable units like those that typify the latter (Stone and others, 1987). Assignment of the rocks at Marble Canyon to the Darwin Canyon Formation is based on the general lithologic similarities with the type section near Darwin despite the absence of a detailed lithostratigraphic correlation. Thin-bedded siltstone to very fine grained sandstone typical of the Panamint Springs Member of the Darwin Canyon Formation, which overlies the Millers Spring Member near Darwin, is not present in the Marble Canyon area.

Detailed studies of the type section of the Millers Spring Member (Lico, 1983; Stone, 1984; Stevens and others, 1989) have led to the conclusion that most of the rocks in this unit originated as sediment-gravity-flow deposits in a deep-water basin. In its type area, the Millers Spring Member contains numerous thick, graded, bioclastic to conglomeratic limestone beds that clearly originated as turbidites, as well as two thick, massive beds of very fine grained silty limestone with matrix-supported clasts interpreted as submarine debris-flow deposits. The associated siliciclastic siltstone to very fine grained sandstone in the type Millers Spring Member forms even, laterally extensive beds, commonly separated by mudstone, that are characterized by pervasive planar and cross lamination and locally contain various types of sole marks. Stone (1984) noted that these sedimentary features resemble those in sandstone beds of the Permian Basin of west Texas that have been interpreted as nonturbid density flows laid down by currents charged by hypersaline water (Harms, 1974; Williamson, 1979). Alternatively, Stevens and others (1989) interpreted these beds to have been deposited by moderate-density turbidity currents based on comparison with sediment-gravity-flow models discussed by Lowe (1982). Both interpretations imply a relatively deep-water depositional environment.

The generally similar rocks assigned to the Darwin Canyon Formation at Marble Canyon probably represent similar modes of sediment-gravity-flow deposition, although the evidence for this is not as clear in this area as it is near Darwin. At Marble Canyon, graded limestone beds are uncommon and bedding in the siltstone to very fine grained sandstone is largely obscured by the lack of interlayered mudstone. The thick, massive bed of clast-bearing silty limestone near the top of the Darwin Canyon Formation at Marble Canyon, however, clearly is a debris-flow deposit like those present near Darwin, and the thinner clastic limestone beds in the section are presumably turbidites even though most are not graded. The rare presence of radiolarian chert also points to a deep-water environment.

Conodonts from three limestone samples between 125 and 247 m above the base of the Darwin Canyon Formation in measured section MC-2 indicate an Artinskian (early Permian) age (appendix 3). Conodonts in the highest sample (MC-2A-3) suggest a late Artinskian age. By contrast, fusulinids and corals from the debris-flow deposit near the top of the Darwin Canyon Formation (appendixes 4, 5) indicate an older age of middle to late Wolfcampian (late Sakmarian to early Artinskian).

Possible Implication of the Permian Conodont Age Interpretations

The ages of rocks assigned to the Osborne Canyon and Darwin Canyon formations based on different fossil groups differ considerably. At Marble Canyon, conodonts from the upper part of the Osborne Canyon Formation and from the Darwin Canyon Formation indicate an Artinskian age, with latest Artinskian conodonts appearing about 250 m above the base of the Darwin Canyon Formation. By contrast, near Darwin, fusulinids reported by Magginetti and others (1988) indicate a middle Wolfcampian (Sakmarian) age for the Osborne Canyon Formation and a middle to late Wolfcampian (late Sakmarian to middle Artinskian) age for the Millers Spring Member of the Darwin Canyon Formation, which corresponds lithologically to the Darwin Canyon Formation at Marble Canyon. Moreover, both fusulinids and corals from the debris-flow deposit near the top of the Darwin Canyon Formation at Marble Canyon are similar to those from the Millers Spring Member near Darwin, indicating a late Sakmarian to early Artinksian age. These contrasts in age raise the possibility that the fusulinids and corals in the Darwin area and in the debris-flow deposit at Marble Canyon are reworked from older beds.

To investigate this possibility, we searched for conodonts in several limestone samples from the Osborne Canyon and Darwin Canyon Formations near Darwin as part of this study. Of the samples processed, only two (both from the Osborne Canyon Formation) yielded identifiable conodonts. Examination of these conodonts by Wardlaw indicates a fauna dominated by the genus *Rabeignathus*, which does not have a well-constrained stratigraphic range but is likely at least as young as the Permian

faunas at Marble Canyon. We therefore suggest that the corals and fusulinids are, in fact, reworked. Thus, the ages assigned here are based primarily on the interpreted ages of the conodont faunas.

Late Paleozoic Depositional and Paleogeographic History

Mississippian and Pennsylvanian rocks in the Marble Canyon area represent deposition on the western continental shelf of North America, whereas the Permian rocks represent basinal deposition triggered by tectonic activity that caused the shelf to subside (Stevens and others, 1995; Stone and Stevens, 1988; Stevens and Stone, 2007; Martin and others, 2012). Here we review the depositional and paleogeographic history of these upper Paleozoic strata.

Mississippian limestone units at Marble Canyon accumulated on the outer part of a broad carbonate platform that extended southwest across Nevada into east-central California (Belasky, 1988; Stevens and others, 1995). Evolution of the Mississippian platform was controlled by a combination of tectonic subsidence due to thrust emplacement of the Roberts Mountains allochthon to the west, carbonate production rates, and eustatic sea-level changes (Poole and Sandberg, 1977, 1991; Sandberg, 2002). Deposition of the Tin Mountain Limestone began in middle Kinderhookian time in response to a major eustatic rise (Sandberg, 2002). Following final emplacement of the Roberts Mountains allochthon, the platform deepened early in middle Osagean time, resulting in deposition of the chert-rich lower member of the Stone Canyon Limestone. This second major Mississippian eustatic rise (Sandberg, 2002) is marked regionally by the Stone Canyon Limestone and the coeval, chert-rich Anchor Member of the Monte Cristo Limestone in Nevada and Thunder Springs Member of the Redwall Limestone in Arizona. These three units represent deep-water outer-platform and upper-slope or upper-ramp settings. In response to a late Osagean eustatic fall, carbonate production increased and a shallow-water carbonate platform began to prograde westward, resulting in deposition of the upper member of the Stone Canyon Limestone and the Santa Rosa Hills Limestone, which continued into Meramecian time. Coeval basin sediments were deposited west of the Meramecian (early Late Mississippian) platform margin (fig. 5*A*).

The disconformable contact between the Santa Rosa Hills Limestone and the overlying Indian Springs Formation represents two separate events. First, pronounced shoaling caused the cessation of carbonate sedimentation and local development of a lycopsid forest on the upper surface of the Santa Rosa Hills Limestone (Decourten and Bovee, 1986). This event probably coincided with a major eustatic sea-level fall that has been interpreted to record the onset of late Paleozoic glaciation in southern Gondwana (Bishop and others, 2009). Subsequent widespread deepening led to deposition of the mixed siliciclastic and calcareous sediments of the Chesterian Indian Springs Formation (Poole and Sandberg, 1991) and its deep-water equivalent to the west, the Rest Spring Shale (Titus, 2000). The change from shale in the lower part of the Indian Springs Formation to cross-bedded sandstone in the upper part suggests an overall shallowing trend within the formation at Marble Canyon.

Marine transgression that coincided with a rise in eustatic sea level at about the Mississippian-Pennsylvanian boundary (Ross and Ross, 1987) led to establishment of the Bird Spring carbonate platform (Stevens and Stone, 2007), which covered most of the area previously occupied by the Mississippian platform. Analysis of regional sedimentary facies patterns indicates that the Bird Spring Platform did not extend as far southwest as the older Mississippian platform (Stone, 1984). Instead, the margin of the Bird Spring Platform, flanked on the west by the deep-water Keeler Basin (Stevens and others, 2001), changed from a southwesterly to a southeasterly orientation in the vicinity of Panamint Valley (fig. 5*B*). This change in the trend of the platform margin reflects subsidence of the southwestern part of the former Mississippian carbonate platform, which is interpreted to have resulted from tectonic deformation related to Pennsylvanian truncation of the continental margin along a southeast-trending

transform fault zone (Stone and Stevens, 1988). Marble Canyon represents a position on the outer part of the Bird Spring Platform almost directly east of the bend in the platform margin (fig. 5*B*).

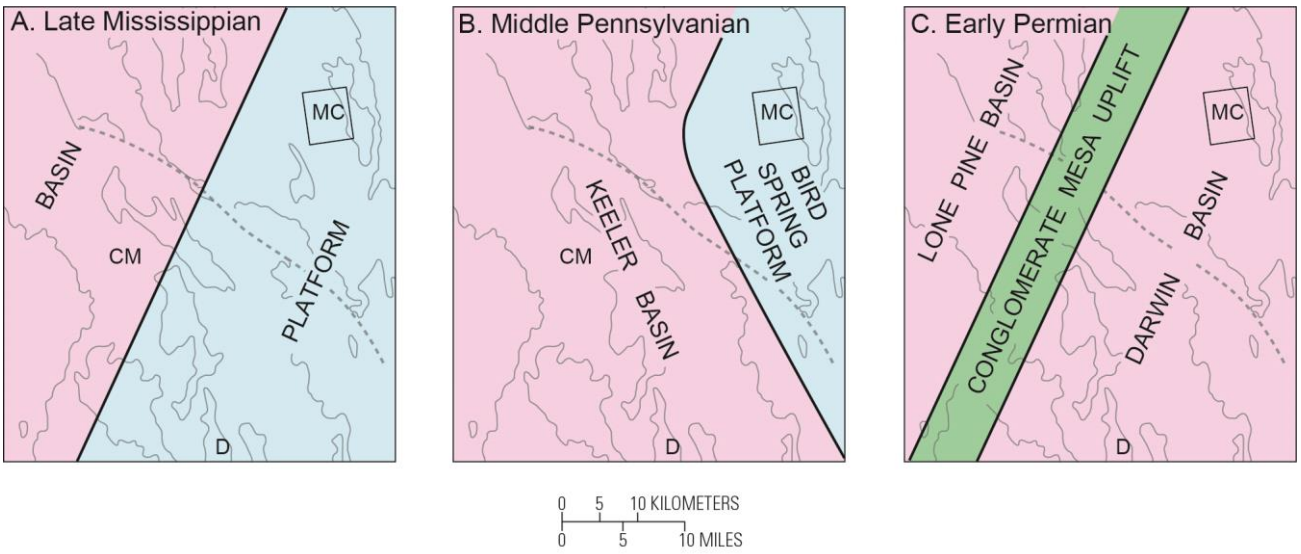

Figure 5. Maps illustrating Mississippian to Permian paleogeographic evolution of the Inyo Mountains-Cottonwood Mountains area. Rectangle in northeastern part of each map denotes area of geologic map; range outlines are the same as on figure 1. Dotted line is trace of Hunter Mountain Fault, on which 10 km of right-lateral displacement has been restored based on the interpretations of Burchfiel and others (1987). Note that this restoration caused slight counter-clockwise rotation of the geologic map area. See text for discussion of paleogeographic evolution. CM, Conglomerate Mesa; D, Darwin; MC, Marble Canyon.

The Bird Spring Formation at Marble Canyon makes up the outer platform component of ten third-order (1 to 5 m.y. duration) stratigraphic sequences recently defined for the regional platform succession (Greene, 2010; Martin and others, 2012; fig. 6). Sequence 1, which developed during the early stages of the marine transgression, probably is represented by the early Morrowan hiatus or condensed section that underlies the Bird Spring Formation. The overlying fine-grained calcareous turbidites of member 1 of the Bird Spring Formation are interpreted as a transgressive systems tract deposited during a major rise in relative sea level marking the base of sequence 2. These turbidites were presumably derived from coeval, shallow-water, inner-platform banks to the east. The hiatus or condensed section below member 1 may represent an area of sediment bypass during earlier turbidite deposition farther offshore. Morrowan to Desmoinesian micritic limestone and calcisiltite of member 2 comprise the outer-platform to upper-slope component of regional sequences 2–6. Discrete intervals of contorted limestone exhibiting soft-sediment deformation and lateral monomictic breccia are interpreted as the outermost platform expression of sequence boundaries (Martin and others, 2012) given that the platform-margin carbonates would have been most unstable during periods of lowered sea level (Yose and Heller, 1989; Catuneanu and others, 2009). Shoaling toward the end of member 2 deposition, followed by the appearance of thick-bedded to massive, skeletal limestone in member 3, marks a short-lived fall in relative sea level at the top of sequence 6 and westward progradation of inner-platform facies into the Marble Canyon area (Martin and others, 2012). The return to predominantly micritic limestone deposition in member 4 is interpreted to record a gradual long-term rise in relative sea level that generally corresponds to a similar sea-level rise recognized in Upper Pennsylvanian cyclothemic successions in paleotropical basins of central and eastern Pangaea (Eros and others, 2012a, b). Member 4 is interpreted to represent sequences 7 and 8 of the regional platform succession. Sequences 9 and 10

are probably missing at Marble Canyon across the disconformable contact between the Bird Spring and Osborne Canyon Formations (fig. 6).

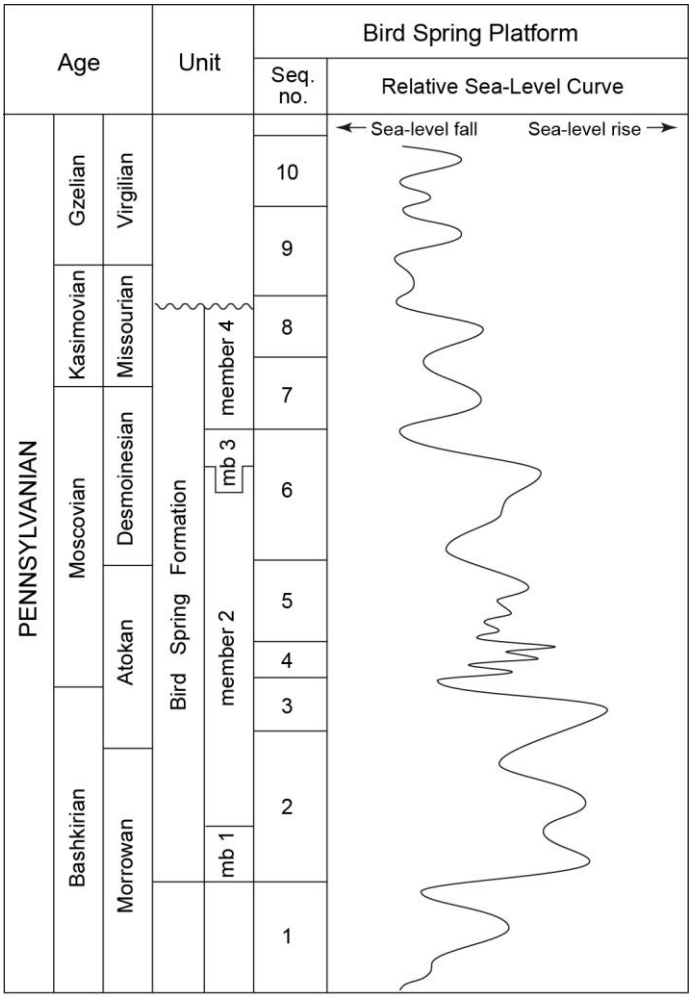

Figure 6. Chart showing correlation of members 1–4 of the Bird Spring Formation at Marble Canyon with regional stratigraphic sequences and relative sea-level curve for the Bird Spring Platform (modified from Martin and others, 2012).

The regional paleogeography was fundamentally changed by major tectonic activity along the continental margin beginning in middle early Permian time. Southeast-vergent thrust faulting and folding near the eastern margin of the Keeler Basin, interpreted to be related to emplacement of the Last Chance thrust plate (Stewart and others, 1966; Stevens and Stone, 2005a), formed a northeast-trending structural ridge called the Conglomerate Mesa Uplift (fig. 5*C*). Simultaneous downwarping to the east caused widespread subsidence of the Bird Spring Platform and eastward migration of the shelf edge (Stevens and Stone, 2007). Early Permian sedimentation that postdated initiation of this deformation took place in the deep-water Lone Pine and Darwin Basins that flanked the Conglomerate Mesa Uplift on its northwest and southeast sides, respectively (fig. 5*C*; Stone and Stevens, 1988; Stevens and Stone, 2007). The Marble Canyon area was part of the Darwin Basin in which the regionally extensive, deep-water strata of the Osborne Canyon and Darwin Canyon formations were deposited. Based on the characteristics of these formations in their type area near Darwin, Stone and others (1987) interpreted the Osborne Canyon Formation as a channeled slope sequence and the Darwin Canyon Formation as an

unchanneled basin-floor sequence. The erosional base of the Osborne Canyon Formation at Marble Canyon supports the interpretation that this unit was deposited on a channeled slope. Bioclastic turbidites in both formations are interpreted to have been derived from the Bird Spring Platform to the east, whereas the fine-grained siliciclastic silt and very fine sand that is especially abundant in the Darwin Canyon Formation was likely derived from cratonal sources and possibly transported into the basin through channels cut into the carbonate platform (Stevens and others, 1989).

Deformation and sedimentation along the western margin of the Darwin Basin continued into late Permian time as observed in the Inyo Mountains near Conglomerate Mesa (Stone and others, 2009). The culminating phase of this deformation was part of the regionally extensive Sierra Nevada-Death Valley Thrust System of late Permian age (Stevens and Stone, 2005b), which is interpreted to have included the Marble Canyon Thrust Fault just west of the present map area.

References Cited

Belasky, P., 1988, Stratigraphy and paleogeographic setting of the Mississippian Monte Cristo Group in the Spring Mountains, Nevada: San Jose, Calif., San Jose State University, M.S. thesis, 156 p.

Bishop, J.W., Montañez, I.P., Gulbranson, E.L., and Brenckle, P.L., 2009, The onset of mid-Carboniferous glacio-eustacy—Sedimentologic and diagenetic constraints, Arrow Canyon, Nevada: Palaeogeography, Palaeoclimatology, Palaeocology, v. 276, p. 217–243.

Burchfiel, B.C., Hodges, K.V., and Royden, L.H., 1987, Geology of Panamint Valley-Saline Valley pull-apart system, California—Palinspastic evidence for low-angle geometry of a Neogene range-bounding fault: Journal of Geophysical Research, v. 92, no. B10, p. 10,422–10,426.

Catuneanu, O., Abreu, V., Bhattcharya, J.P., and 25 others, 2009, Towards the standardization of sequence stratigraphy: Earth-Science Reviews, v. 92, no. 1–2, p. 1–33.

Clark, D.L., Sweet, W.C., Bergström, S.M., Klapper, G., Austin, R.L., Rhodes, F.H.T., Müller, K.J., Ziegler, W., Lindström, M., Miller, J.G., and Harris, A.G., 1981, Conodonta, *in* Robison, R.A., ed., Treatise on Invertebrate Paleontology, pt. W supplement 2: Geological Society of America and Kansas University, p. W1–W202.

Davydov, V., Wardlaw, B.R., and Gradstein, F.M., 2004, The Carboniferous Period, chap. 15 *of* Gradstein, F.M., Ogg, J.G., and Smith, A.G., eds., A geologic time scale 2004: Cambridge, UK, Cambridge University Press, p. 222–248.

Decourten, F.L., and Bovee, B., 1986, *Stigmaria* from the upper Carboniferous Rest Spring Shale and a possible *Lepidodendrale* rooting ground, Death Valley region, SE California [abs.]: Geological Society of America Abstracts with Programs, v. 18, no. 2, p. 100.

Dunne, G.C., Gulliver, R.M., and Stevens, C.H., 1981, Correlation of Mississippian shelf-to-basin strata, eastern California: Geological Society of America Bulletin, Part II, v. 92, p. 1–38.

Eros, J.M., Montañez, I.P., Osleger, D.A., Davydov, V.I., Nemyrovska, T., Poletaev, V., and Zhykalyak, M.V., 2012a, Sequence stratigraphy and onlap history of the Donets Basin, Ukraine—Insight into Carboniferous icehouse dynamics: Palaeogeography, Palaeoclimatology, Palaeoecology, v. 313–314, p. 1–25.

Eros, J.M., Montañez, I.P., Osleger, D.A., Davydov, V.I., Nemyrovska, T., Poletaev, V., and Zhykalyak, M.V., 2012b, Reply to the comment on “Sequence stratigraphy and onlap history of the Donets Basin, Ukraine—Insight into Carboniferous icehouse dynamics”: Palaeogeography, Palaeoclimatology, Palaeoecology, v. 363–364, p. 187–191.

Greene, L.E., 2010, A paleotropical carbonate-dominated archive of late Paleozoic icehouse dynamics, Bird Spring Fm., southern Great Basin, USA: Davis, University of California, M.S. thesis, 126 p.

Harms, J.C., 1974, Brushy Canyon Formation, Texas—A deep-water density current model: Geological Society of America Bulletin, v. 85, p. 1763–1784.

Hewett, D. F., 1931, Geology and ore deposits of the Goodsprings quadrangle, Nevada: U.S. Geological Survey Professional Paper 162, 172 p.

Jennings, C.W., 1977, Geologic map of California: California Division of Mines and Geology, scale 1:750,000.

Johnson, E.A., 1971, Geology of a part of the southeastern side of the Cottonwood Mountains, Death Valley, California: Houston, Texas, Rice University, Ph.D dissertation, 81 p.

Klingman, D.S., 1987, Depositional environments and paleogeographic setting of the middle Mississippian section in eastern California: San Jose, Calif., San Jose State University, M.S. thesis, 231 p.

Knott, J.R., Machette, M.N., Klinger, R.E., Sarna-Wojcicki, A.M., Liddicoat, J.C., Tinsley, J.C., III, David, B.T., and Ebbs, V.M., 2008, Reconstructing late Pliocene to middle Pleistocene Death Valley lakes and river systems as a test of pupfish (*Cyprinodontidae*) dispersal hypotheses, *in* Reheis, M.C., Hershler, R., and Miller, D.M., eds., Late Cenozoic drainage history of the southwestern Great Basin and lower Colorado River region—Geologic and biotic perspectives: Geological Society of America Special Paper 439, p. 1–26.

Knott, J.R., Sarna-Wojcicki, A.M., Meyer, C.E., Tinsley, J.C., III, Wells, S.G., and Wan, E., 1999, Late Cenozoic stratigraphy and tephrochronology of the western Black Mountain piedmont, Death Valley, California—Implications for the tectonic development of Death Valley, *in* Wright, L.A., and Troxel, B.W., eds., Cenozoic basins of the Death Valley region: Geological Society of America Special Paper 333, p. 345–366.

Lane, H.R., Brenckle, P.L., Baesemann, J.F., and Richards, B., 1999, The IUGS boundary in the middle of the Carboniferous—Arrow Canyon, Nevada, USA: Episodes, v. 22, p. 272–283.

Lane, H.R., Sandberg, C.A., and Ziegler, W., 1980, Taxonomy and phylogeny of some Lower Carboniferous conodonts and preliminary standard post-*Siphonodella* zonation: Geologica et Paleontologica, v. 14, p. 117–164.

Lee, C., 1975, Lower Permian ammonoid faunal provinciality: Iowa City, University of Iowa, Ph.D dissertation, 252 p.

Lico, M.S., 1983, Lower Permian submarine sediment gravity flows in the Owens Valley Formation, southeastern California: San Jose, Calif., San Jose State University, M.S. thesis, 80 p.

Lowe, D.R., 1982, Sediment gravity flows II—Depositional models with special reference to the deposits of high-density turbidity currents: Journal of Sedimentary Petrology, v. 52, p. 279–297.

Magginetti, R.T., Stevens, C.H., and Stone, P., 1988, Early Permian fusulinids from the Owens Valley Group, east-central California: Geological Society of America Special Paper 217, 61 p.

Martin, L.G., Montañez, I.P., and Bishop, J.W., 2012, A paleotropical carbonate-dominated archive of Carboniferous icehouse dynamics, Bird Spring Formation, southern Great Basin, USA: Palaeogeography, Palaeoclimatology, Palaeoecology, v. 329–330, p. 64–82.

McAllister, J.F., 1952, Rocks and structure of the Quartz Spring area, northern Panamint Range, California: California Division of Mines Special Report 25, 38 p.

McAllister, J.F., 1956, Geology of the Ubehebe Peak quadrangle, California: U.S. Geological Survey Geologic Quadrangle Map GQ-95, scale 1:62,500.

McAllister, J.F., 1974, Silurian, Devonian, and Mississippian formations in the Ryan quadrangle, Death Valley region, California: U.S. Geological Survey Bulletin 1386, 35 p.

Merriam, C.W., 1963, Geology of the Cerro Gordo mining district, Inyo County, California: U.S. Geological Survey Professional Paper 408, 83 p.

Poole, F.G., and Sandberg, C.A., 1977, Mississippian paleogeography and tectonics of the western United States, *in* Stewart, J.H., Stevens, C.H., and Fritsche, A.E., eds., Paleozoic paleogeography of the western United States: Los Angeles, Calif., Society of Economic Paleontologists and Mineralogists, Pacific Section, p. 67–85.

Poole, F.G., and Sandberg, C.A., 1991, Mississippian paleogeography and conodont biostratigraphy of the western United States, *in* Cooper, J.D., and Stevens, C.H., eds., Paleozoic paleogeography of the western United States—II: Los Angeles, Calif., Society of Economic Paleontologists and Mineralogists, Pacific Section, v. 1, p. 107–136.

Ross, C.A., and Ross, J.R.P., 1987, Late Paleozoic sea levels and depositional sequences: Washington, D.C., Smithsonian Institution Cushman Foundation for Foraminiferal Research, Special Publication 24, p. 137–149.

Sandberg, C.A., 2002, Mississippian: McGraw-Hill Encyclopedia of Science & Technology, 9th ed., v. 11, p. 254–257.

Sandberg, C.A., and Gutschick, R.C., 1984, Distribution, microfauna, and source-rock potential of Mississippian Delle Phosphatic Member of Woodman Formation and equivalents, Utah and adjacent states, *in* Woodward, J., Meissner, F.F., and Clayton, J.L., eds., Hydrocarbon source rocks in the greater Rocky Mountain region: Denver, Colo., Rocky Mountain Association of Geologists, p. 135–178.

Sando, W.J., 1980, The paleoecology of Mississippian corals in the western conterminous United States: Acta Palaeontologica Polonica, v. 25, p. 619–631.

Sarna-Wojcicki, A.M., Reheis, M.C., Pringle, M.S., Fleck, R.J., Burbank, D., Meyer, C.E., Slate, J.L., Wan, E., Budahn, J.R., Troxel, B., and Walker, J.P., 2005, Tephra layers of Blind Spring Valley and related upper Pliocene and Pleistocene tephra layers, California, Nevada, and Utah—Isotopic ages, correlation, and magnetostratigraphy: U.S. Geological Survey Professional Paper 1701, 63 p.

Snow, J.K., 1990, Cordilleran orogenesis, extensional tectonics, and geology of the Cottonwood Mountains area, Death Valley region, California and Nevada: Cambridge, Mass., Harvard University, Ph.D dissertation, 508 p.

Snow, J.K., 1992, Large-magnitude Permian shortening and continental-margin tectonics in the southern Cordillera: Geological Society of America Bulletin, v. 104, no. 1, p. 80–105.

Snow, J.K., and Lux, D.R., 1999, Tectono-sequence stratigraphy of Tertiary rocks in the Cottonwood Mountains and northern Death Valley area, California and Nevada, *in* Wright, L.A., and Troxel, B.W., eds., Cenozoic basins of the Death Valley region: Geological Society of America Special Paper 333, p. 17–64.

Snow, J.K., and Wernicke, B.P., 2000, Cenozoic tectonism in the central Basin and Range—Magnitude, rate, and distribution of upper crustal strain: American Journal of Science, v. 300, p. 659–719.

Stadler, C.A., 1968, The geology of the Goldbelt Spring area, northern Panamint Range, Inyo County, California: Eugene, University of Oregon, M.S. thesis, 78 p.

Stevens, C.H., 1995, A new Middle Pennsylvanian species of *Petalaxis* (Rugosa) from eastern California: Journal of Paleontology, v. 69, no. 4, p. 787–789.

Stevens, C.H., Klingman, D., and Belasky, P., 1995, Development of the Mississippian carbonate platform in southern Nevada and eastern California on the eastern margin of the Antler foreland basin, *in* Dorobek, S.L., and Ross, G.M., eds., Stratigraphic evolution of foreland basins: Society for Sedimentary Geology Special Publication 52, p. 175–186.

Stevens, C.H., Klingman, D.S., Sandberg, C.A., Stone, P., Belasky, P., Poole, F.G., and Snow, J.K., 1996, Mississippian stratigraphic framework of east-central California and southern Nevada with revision of Upper Devonian and Mississippian stratigraphic units in Inyo County, California: U.S. Geological Survey Bulletin 1988–J, p. J1–J39.

Stevens, C.H., Lico, M.S., and Stone, P., 1989, Lower Permian sediment-gravity-flow sequence, eastern California: Sedimentary Geology, v. 64, p. 1–12.

Stevens, C.H., and Stone, P., 2005a, Interpretation of the Last Chance thrust, Death Valley region, California, as an Early Permian décollement in a previously undeformed shale basin: Earth-Science Reviews, v. 73, p. 79–101.

Stevens, C.H., and Stone, P., 2005b, Structure and regional significance of the Late Permian(?) Sierra Nevada-Death Valley thrust system, east-central California: Earth-Science Reviews, v. 73, p. 103–113.

Stevens, C.H., and Stone, P., 2007, The Pennsylvanian–Early Permian Bird Spring carbonate shelf, southeastern California—Fusulinid biostratigraphy, paleogeographic evolution, and tectonic implications: Geological Society of America Special Paper 429, 82 p.

Stevens, C.H., Stone, P., and Ritter, S.M., 2001, Conodont and fusulinid biostratigraphy and history of the Pennsylvanian to Lower Permian Keeler Basin, east-central California: Brigham Young University Geology Studies, v. 46, p. 99–142.

Stewart, J.H., Ross, D.C., Nelson, C.A., and Burchfiel, B.C., 1966, Last Chance thrust—A major fault in the eastern part of Inyo County, California: U.S. Geological Survey Professional Paper 550-D, p. D23–D34.

Stewart, J.H., Sarna-Wojcicki, A., Meyer, C.E., and Wan, E., 1999, Stratigraphy, tephrochronology, and structural setting of Miocene sedimentary rocks in the Cobble Cuesta area, west-central Nevada: U.S. Geological Survey Open-File Report 99–352, 21 p.

Stone, P., 1984, Stratigraphy, depositional history, and paleogeographic significance of Pennsylvanian and Permian rocks in the Owens Valley-Death Valley region, California: Stanford, Calif., Stanford University, Ph.D dissertation, 399 p.

Stone, P., and Stevens, C.H., 1984, Stratigraphy and depositional history of Pennsylvanian and Permian rocks in the Owens Valley-Death Valley region, eastern California, *in* Lintz, Joseph, Jr., ed., Western geological excursions, Volume 4—Geological Society of America annual meeting guidebook: Reno, Nevada, Mackay School of Mines, p. 94–119.

Stone, P., and Stevens, C.H., 1988, Pennsylvanian and Early Permian paleogeography of east-central California—Implications for the shape of the continental margin and the timing of continental truncation: Geology, v. 16, p. 330–333.

Stone, P., Stevens, C.H., and Magginetti, R.T., 1987, Pennsylvanian and Permian stratigraphy of the northern Argus Range and Darwin Canyon area, California: U.S. Geological Survey Bulletin 1691, 30 p.

Sweet, W.C., 1988, The Conodonta—Morphology, taxonomy, paleoecology, and evolutionary history of a long-extinct animal phylum: New York, Oxford, Clarendon Press, Oxford Monographs on Geology and Geophysics, no. 10, 212 p.

Titus, A.L., 2000, Late Mississippian (Arnsbergian Stage-E_2 chronozone) ammonoid paleontology and biostratigraphy of the Antler foreland basin, California, Nevada, Utah: Utah Geological Survey Bulletin 131, 109 p.

Wardlaw, B.R., Davydov, V., and Gradstein, F.M., 2004, The Permian Period, chap. 16 *of* Gradstein, F.M., Ogg, J.G., and Smith, A.G., eds., A geologic time scale 2004: Cambridge, UK, Cambridge University Press, p. 249–270.

Williamson, C.R., 1979, Deep-sea sedimentation and stratigraphic traps, Bell Canyon Formation (Permian), Delaware Basin, *in* Sullivan, N.M., ed., Guadalupian Delaware Mountain Group of west Texas and southeast New Mexico: Permian Basin Section, Society of Economic Paleontologists and Mineralogists, Publication 79–18, p. 39–74.

Yose, L.A., and Heller, P.L., 1989, Sea-level control of mixed-carbonate-siliciclastic, gravity-flow deposition—Lower part of the Keeler Canyon Formation (Pennsylvanian), southeastern California: Geological Society of America Bulletin, v. 101, no. 3, p. 427–439.

Appendix 1—Measured Sections

All sections are in the Marble Canyon area, Cottonwood Mountains, Death Valley National Park, California (Cottonwood Canyon 7½-minute quadrangle). See geologic map for locations. Coordinates referenced to 1927 North American Datum.

Measured Section CC

Santa Rosa Hills Limestone, Stone Canyon Limestone, and Tin Mountain Limestone. Base of section is in side canyon 1.1 km northwest of junction with Cottonwood Canyon at lat 36°34'45" N., long 117°19'41" W., elevation 2,480 ft. Top of section is on ridge at lat 36°35'07" N., long 117°19'34" W., elevation 3,260 ft. Modified from Cottonwood Canyon section of Belasky (1988).

	Thickness in meters	Cumulative thickness of unit in meters
Indian Springs Formation (Mississippian) (not measured):		
11. Sandstone, shale, and sandy limestone	---	
Santa Rosa Hills Limestone (Mississippian):		
10. Limestone (crinoidal packstone), light- to medium-gray, fine- to medium-grained, medium- to thick-bedded; locally contains calcareous foraminifers. Dark-gray, reddish-brown-weathering chert nodules and lenses form about 10 percent of unit and are most abundant near base	68	109
9. Limestone (crinoidal wackestone and packstone), medium-gray, massive. Dark-gray, reddish-brown- to black-weathering chert nodules and lenses that occur in thin, regularly spaced, laterally persistent layers form about 20 percent of unit	4	41
8. Limestone (crinoidal wackestone, packstone, and grainstone), light-gray, fine- to coarse-grained, thick-bedded. Crinoidal debris ranges in size from fine sand to gravel. Dark-gray, black- to reddish-brown-weathering chert nodules form less than 2 percent of unit. Conodont sample CC-6 from about 16 m above base of unit	37	37
Total thickness of Santa Rosa Hills Limestone	109	
Stone Canyon Limestone (Mississippian):		

Upper member (units 7–6, total thickness 116 m):

7. Limestone (crinoidal packstone) (50 percent): medium-gray, predominantly coarse-grained, medium- to thick-bedded; graded beds common; becomes more abundant and thicker bedded in upper part of unit. Limestone (lime mudstone and wackestone) (30 percent): medium- to dark-gray, predominantly fine-grained, thin- to medium-bedded, finely laminated, commonly silicified; contains crinoids, fenestrate bryozoans (commonly oriented parallel to bedding), and rare syringoporoid corals; most abundant in lower part of unit. Chert lenses and nodules (20 percent): gray, weathers reddish brown; most abundant in lower part of unit. Fasciculate rugose corals (sample PD1) present 23 m below top of unit; conodont sample CC-4 from about 50 m below top of unit 75 417

6. Limestone (lime mudstone and wackestone) (50 percent): dark-gray, predominantly fine-grained, thin- to medium-bedded, some finely laminated. Limestone (crinoidal packstone and grainstone) (25 percent): gray, medium- to coarse-grained, thin- to medium-bedded; commonly exhibits crude graded bedding; gradually increases in abundance toward top of unit. Chert nodules, lenses, and beds (25 percent): dark-gray to black, weathers reddish brown; commonly occurs in regularly spaced, laterally persistent layers 41 342

Lower member (units 5–3, total thickness 301 m):

5. Limestone (lime mudstone and wackestone) (50 percent): dark-gray, predominantly fine-grained, medium- to thick-bedded, commonly silicified. Chert nodules, lenses, and beds (50 percent): dark-gray to black, weathers black to dark reddish gray, variable in thickness; commonly occurs in regularly spaced, laterally persistent layers; some layers are lenticular, wavy, and irregular; often blocky on weathered surfaces. Macrofossils rare. Conodont sample CC-1 from 41 m below top of unit 76 301

4. Limestone (lime mudstone and wackestone) (50 percent): dark-gray, fine-grained, predominantly thin-bedded, commonly silicified; some contains scattered crinoids, solitary rugose corals, and sponge spicules. Chert nodules, lenses, and beds (50 percent): dark-gray to black, weathers dark reddish brown; predominantly thin-bedded, commonly lenticular; blocky on weathered surfaces; resistant; most abundant towards base of unit 185 225

3. Limestone (lime mudstone and wackestone) (50 percent): dark-gray, some medium-gray near base of unit, predominantly fine-grained, thin- to medium-bedded, sparsely fossiliferous, commonly silicified. Chert nodules, lenses, and beds (50 percent): dark-gray to black, weathers dark reddish brown; thin- to thick-bedded, commonly lenticular, wavy, irregular; blocky

on weathered surfaces; resistant. Conodont sample PD17 from 1 m above base of unit	40	40
Total thickness of Stone Canyon Limestone	417	
Tin Mountain Limestone (Mississippian) (incomplete):		
2. Limestone (crinoidal wackestone and packstone), dark-gray, fine- to medium-grained, predominantly medium-bedded; forms resistant cliffs. Contains crinoid debris, bryozoans, brachiopods, and solitary rugose corals. Crinoidal debris most abundant near top of unit. Interbedded dark-gray, light-red-weathering lime mudstone locally forms very thin, continuous partings. Black chert nodules form as much as 10 percent of unit	37	40
1. Limestone (lime mudstone and wackestone), medium- to dark-gray, predominantly fine-grained, medium-bedded; contains scattered crinoid debris, bryozoans, brachiopods, solitary rugose corals, and sponge spicules. Interbedded dark-gray, light-red- to reddish-brown-weathering lime mudstone forms very thin lenses and partings. Black chert nodules form as much as 5 percent of unit	3	3
Incomplete thickness of Tin Mountain Limestone	40	
Base of section covered.		

Measured Section MC-1

Bird Spring Formation and Indian Springs Formation. Section is in Marble Canyon. Base of section is at lat 36°36'19" N., long 117°20'08" W., elevation 2,160 ft; top of section is at lat. 36°37'11" N., long 117°19'43" W., elevation 1,960 ft. Measured by Paul Stone in 1980.

	Thickness in meters	Cumulative thickness of unit in meters
Top of section covered, but probably only a few meters below base of the Osborne Canyon Formation (Permian).		
Bird Spring Formation (Pennsylvanian):		
Member 4 (units 96–85, total thickness 107.9 m):		
96. Limestone, forming a massive ledge. Lower 3 m is light-gray silty limestone, in part laminated, interbedded with thin partings of buff, laminated siltstone. Limestone in beds 10–30 cm thick. Upper 3 m is massive crinoidal limestone (wackestone and packstone) containing scattered lenses and nodules of brown chert 0.5 m long. Thin-section sample MC-1-55 (crinoidal limestone) from upper part of unit	6.0	601.3
95. Interval largely covered. Rare outcrops of evenly laminated silty limestone and calcareous siltstone that weather buff to 1ight gray	3.0	595.3
94. Limestone, forming a massive ledge. Lower 2 m is light- to medium-gray crinoidal limestone (packstone). Upper 3 m is dark-gray micritic limestone containing irregular brown chert		

nodules and lenses. Conodont sample MC-1-53 from base of unit	5.0	592.3
93. Interbedded buff silty limestone (75 percent) and light- to medium-gray limestone (25 percent), both micritic. Buff limestone contains abundant aligned nodules of brown chert	15.0	587.3
92. Interbedded buff silty limestone (50 percent) and light- to medium-gray limestone (50 percent), both micritic. Buff limestone contains abundant nodules, lenses, and thin (5–15 cm) beds of brown chert. Gray limestone beds lack chert, but commonly are bounded above and below by chert beds. Conodont sample MC-1-52 from base of unit	7.5	572.3
91. Interbedded buff silty limestone (65 percent) and light- to medium-gray limestone (35 percent), both micritic. Beds 20–50 cm thick. Buff limestone contains abundant nodules and lenses of brown chert	14.0	564.8
90. Limestone, micritic, silty, buff to purplish-gray, massive; locally contains aligned chert nodules. Chert abundant in lower meter	11.0	550.8
89. Limestone, micritic, light- to medium-gray; beds 30–60 cm thick. Beds separated by thin partings of buff silty limestone. Contains rare, irregular chert nodules. Locally contains laminae of fossil debris to coarse sand size. Conodont sample MC-1-51 from 1 m above base of unit	3.2	539.8
88. Interbedded buff silty limestone (75 percent) and light- to medium-gray limestone (25 percent), both micritic. Buff limestone beds 50 cm to 1 m thick; gray limestone beds 15–30 cm thick. Buff limestone contains aligned chert nodules. Gray limestone beds generally lack chert but commonly are bounded above and below by cherty layers	14.0	536.6
87. Limestone, forming a massive ledge. Lower 1.5 m is dark-gray micritic limestone. Overlying 3 m is crinoidal limestone (wackestone and packstone) that contains 30 percent irregularly bedded chert in layers 1–8 cm thick. Upper 3 m is crinoidal limestone (packstone) that contains small solitary rugose corals near top. Unit pinches out within 50 m along strike in both directions from line of section. Conodont sample MC-1-49 from base of unit	7.5	522.6
86. Limestone, micritic, silty, purplish-gray in lower half and light-gray in upper half. Aligned, irregular chert nodules locally abundant. Locally contains fossil debris to coarse sand size, particularly near base	7.2	515.1
85. Limestone, micritic, silty, buff to pinkish-gray. Contains abundant, large, irregular nodules of brown chert that are aligned in planar concentrations. Locally contains planar concentrations of fossil debris, most1y crinoidal. Thin-section sample MC-1-48 from 1 m below top of unit	14.5	507.9
Member 3 (units 84–73, total thickness 75.7 m):		
84. Limestone, medium- to dark-gray, massive. Micritic limestone and wackestone in lower part grade upward to crinoidal		

packstone. Central part contains two prominent bands of lenticular brown chert. Colonial coral observed on upper bedding surface of unit (coral sample SJS 1073)	5.8	493.4
83. Limestone (crinoidal packstone), light-gray	1.6	487.6
82. Limestone (crinoidal packstone), dark-gray, containing irregular lenses and aligned nodules of chert. Unit pinches out within 30 m along strike from 1ine of section	0.7	486.0
81. Limestone, micritic, silty; light-gray, buff, and pinkish-gray; massive. Contains abundant lenticular and nodular chert	2.6	485.3
80. Limestone (crinoidal wackestone and packstone), light- to dark-gray, massive. Fusulinids present in upper part of unit. Conodont sample MC-1-46 and fusulinid sample S-1508 from 0.4 m below top of unit; also fusulinid sample S-2100 from approximately the same locality	4.6	482.7
79. Limestone, micritic, silty, light-gray in lower part and buff in upper part, faintly bedded. Contains abundant nodules and lenses of brown chert that form planar zones 5–10 cm thick. Conodont sample MC-1-45 from 1 m above base of unit	9.3	478.1
78. Limestone, micritic, gray, containing lenticular and bedded chert. Lowermost 50 cm is purplish-gray silty limestone	3.5	468.8
77. Limestone, forming a massive ledge. Lower 2.4 m is light-gray to pinkish-gray, silty micritic limestone that contains abundant aligned nodules and lenses of black chert. Overlying 2.0 m is dark-gray micritic limestone, also with abundant black chert. Upper 7.0 m is massive wackestone and packstone containing minor chert	11.4	465.3
76. Limestone, micritic, containing rare crinoidal debris. Contains scattered large chert nodules 15–20 cm thick and 75 cm long	1.9	453.9
75. Limestone, micritic, silty, pinkish-gray to light-gray, massive. Uppermost 10 cm is black chert	1.0	452.0
74. Limestone, gray, forming a massive ledge. Lower 4 m is micritic limestone containing rare fossil debris and abundant large nodules and lenses of brown chert. Upper 6 m is massive crinoidal limestone (wackestone and packstone) containing minor chert. Base of unit marked by a few centimeters of pale-pink, silty limestone	10.0	451.0
73. Limestone, dark-gray, massive; dominantly coarse-grained crinoidal packstone; fusulinids present locally. Chert abundant in upper part, particularly the uppermost 1–2 m. Conodont sample MC-1-40 from 1.5 m above base of unit; conodont and thin-section sample MC-1-41 from 9 m above base of unit; conodont sample MC-1-42 and fusulinid sample S-1507 from 20 m above base of unit	23.3	441.0
Member 2: (measured units 72–7, total thickness 379.3 m):		
72. Limestone, micritic, containing scattered coarse crinoidal debris. Nodular and lenticular chert common	2.7	417.7
71. Limestone, micritic, silty, dominantly light-gray; buff to pinkish-gray in uppermost 2 m. Fossil debris (mostly crinoid debris and		

bryozoa) common on exposed bedding planes and throughout uppermost 2 m. Lenticular chert and elongate chert nodules abundant; spherical chert nodules present. Unit massive except for chert banding	11.6	415.0
70. Limestone, micritic, containing very large, irregular chert nodules	0.7	403.4
69. Limestone, micritic, silty, light-gray to light purplish-gray. Coarse crinoid debris, including articulated stems, scattered throughout. Lenticular chert rare, increasing in abundance upward	5.3	402.7
68. Limestone, micritic, silty. Crinoid debris and bryozoa locally abundant. Nodular chert rare. Conodont sample MC-1-37 from 0.5 m below top of unit	3.8	397.4
67. Limestone, micritic, silty, containing planar concentrations of crinoid debris and bryozoa. Chert absent except for nodules in lowermost meter	4.7	393.6
66. Limestone, micritic, silty, buff to pinkish-gray. Lenses of black chert ranging from less than 1 cm to 3 cm thick spaced 2–10 cm apart. Thin-section sample MC-1-35 from near middle of unit	14.0	388.9
65. Limestone, micritic, light-gray, massive, containing rare spherical chert nodules	4.5	374.9
64. Limestone, micritic, light-gray, massive, containing irregular chert nodules. Conodont samp1e MC-l-34	1.5	368.9
63. Limestone, micritic, dark-gray. Chert lenses and beds 1–5 cm thick spaced 5–30 cm apart. Chert light-gray on fresh surfaces, weathers dark brown	3.4	368.9
62. Limestone, micritic, medium-gray, locally containing abundant crinoid debris, bryozoa, gastropods, and fusulinids. Fossil debris commonly forms planar concentrations. Lenses and beds of chert as thick as 10 cm spaced 10–15 cm apart. Spherical and small, irregular chert nodules present in limestone intervals between chert layers. Thin interbeds of purplish-gray silty limestone common in lower 5 m. Conodont and thin-section sample MC-1-33 from a crinoid-rich bed 5 m above base of unit	16.0	365.5
61. Limestone, micritic, silty, pinkish-gray to buff. Beds and lenses of chert 1–2 cm thick spaced 10–40 cm apart. Interbedded with subordinate light- to medium-gray micritic limestone that forms beds 10–20 cm thick. Gray beds commonly bounded above and below by chert layers. Small, spherical chert nodules common throughout unit. Thin-section sample MC-1-31 from middle of unit	41.0	349.5
60. Limestone, micritic, silty, pinkish-gray to buff; similar to 61 but lacks chert. Subordinate light- to medium-gray micritic limestone forms beds 10–15 cm thick	23.0	308.5
59. Limestone, micritic, silty, buff to pinkish-gray, containing laminar concentrations of fossil debris to coarse sand size. Contains rare spherical chert nodules to 2 cm in diameter	2.2	385.5

58. Limestone, micritic, forming alternating light-gray and medium-gray beds 20–50 cm thick. Lenses, elongate nodules, and spherical nodules of chert common in both types of 1imestone	5.9	283.3
57. Limestone, micritic, silty, purplish-gray to buff, laminated. Contains minor thin-bedded chert	4.2	277.4
56. Limestone, micritic, dark-gray, massive, containing scattered fossil debris. Upper bedding surface contains abundant coarse crinoid debris. Unit pinches out within 100 m along strike	4.0	273.2
55. Limestone, micritic, silty, purplish-gray, laminated. Thin-section sample MC-1-27	3.2	269.2
54. Basal 20 cm is purplish-gray, silty micritic limestone; remainder is color-banded cherty limestone as in 53. Conodont sample MC-1-26 from upper 1 m of unit	2.8	266.0
53. Limestone, micritic, forming alternating light-gray and medium-gray beds 20–50 cm thick as in 58. Nodular and lenticular chert common, especially in light-gray beds. Medium-gray beds commonly bounded above and below by cherty layers 1–2 cm thick. Conodont and thin-section sample MC-1-25 from 1 m above base of unit	6.4	263.2
52. Limestone, micritic, silty, purplish- to pinkish-gray, laminated	5.4	256.8
51. Limestone, micritic, silty, buff, containing abundant beds, lenses, and elongate nodules of dark-brown chert 1–2 cm thick. Chert becomes increasingly abundant and well bedded upward within unit	11.5	251.4
50. Limestone, micritic, silty, pinkish- to purplish-gray, containing scattered large, elongate chert nodules to 20 cm long	1.2	239.9
49. Limestone, micritic, silty; purplish-gray, light-gray, and buff; well laminated to nearly massive. Contains planar concentrations of spherical chert nodules averaging 1 cm in diameter, particularly in upper 5–6 m	17.3	238.7
48. Limestone, micritic, silty, pinkish-gray to buff, plane-laminated to massive. Contains abundant beds and lenses of black chert 1–5 m thick. Thin-section sample MC-1-24	6.0	221.4
47. Limestone, micritic, light- to medium-gray. Fossil debris scattered on some exposed bedding planes. Irregular chert nodules common, spherical chert nodules rare	3.6	215.4
46. Cherty micritic limestone as in 44, forming alternating light-gray and medium-gray beds. Chert forms lenses and elongate nodules	3.8	211.8
45. Limestone, micritic, silty, pinkish-gray, laminated; minor medium-gray micritic limestone in beds 5–10 cm thick	1.5	208.0
44. Limestone, micritic, forming alternating light-gray and medium-gray beds 20–50 cm thick. Lenses, irregular nodules, and spherical nodules of chert abundant, particularly in the light-gray beds	32.0	206.5
43. Limestone, micritic, silty, pinkish-gray. Chert rare, increasing in abundance upward	3.5	174.5
42. Limestone, crinoidal, massive	0.4	171.0

41. Limestone, micritic, silty, buff to pinkish-gray, laminated, as in 39. Chert absent	5.5	170.6
40. Limestone, micritic, silty, buff to pinkish-gray, laminated, as in 39 but with more chert. Lenses, elongate nodules, and spherical nodules of chert abundant. Subordinate light- to medium-gray micritic limestone present in upper part of unit	15.5	165.1
39. Limestone, micritic, silty, buff to pinkish-gray, laminated. Chert generally rare but locally abundant in the form of lenses, elongate nodules, and spherical nodules to 2 cm in diameter. One large (2 m long) clast of silty limestone is enclosed within the unit; bedding in the clast is at an angle to bedding in the unit	11.0	149.6
38. Limestone, micritic, containing lenticular and nodular chert. Unit pinches out within a few meters along strike	1.1	138.6
37. Limestone, micritic, silty, purple	0.4	137.5
36. Limestone, micritic, containing abundant beds, irregular nodules, and spherical nodules of chert. Forms massive ledge	2.0	137.1
35. Limestone, micritic, silty, poorly exposed	1.7	135.1
34. Limestone, micritic, silty, light-gray to buff, containing scattered irregular and spherical nodules of black chert. Uppermost 10 cm composed dominantly of elongate chert nodules. One exposed bedding plane contains abundant crinoidal and bryozoan debris. Conodont sample MC-1-18	2.5	133.4
33. Limestone, micritic, silty, buff to purple; elongate black chert nodules common	1.0	130.9
32. Limestone, micritic, gray, containing rare spherical nodules of black chert	1.0	129.9
31. Limestone, micritic, silty, buff to purple. Elongate black chert nodules 5–20 cm long and 3-5 cm thick form planar concentrations	3.4	128.9
30. Limestone, micritic, light-gray, faintly laminated; spherical chert nodules rare	0.4	125.5
29. Limestone, micritic, silty, buff to purple, containing elongate black chert nodules	0.5	125.1
28. Limestone, micritic, light-gray, faintly laminated; contains rare spherical chert nodules to 2 cm in diameter	0.4	124.6
27. Limestone, micritic, silty; purplish-gray, buff, and light-gray; laminated. Thin-section sample MC-1-17	4.1	124.2
26. Limestone, micritic, forming alternating light-gray and medium- to dark-gray beds averaging about 50 cm thick. Spherical nodules to 5 cm in diameter, elongate nodules, and lenses of chert abundant. Chert commonly forms planar concentrations. Unit thickness varies from 9 to 14 m in vicinity of section; thickness reported here is an average. Conodont sample MC-1-16 from 1 m below top of unit	11.5	120.1
25. Limestone, micritic, silty. Chert rare except for irregular nodules in uppermost part. Conodont sample MC-1-15 from 0.5 m below top of unit	2.3	108.6

24. Limestone, micritic, silty, pinkish-gray. Abundant spherical and elongate nodules of black chert form planar concentrations	0.6	106.3
23. Limestone, micritic, medium- to dark-gray. Lenses, elongate nodules, and spherical nodules (1–2 cm in diameter) of black chert common, increasing in abundance upward	5.5	105.7
22. Limestone, micritic, silty, buff to pinkish-gray, laminated. Thin-section sample MC-1-14	14.6	100.2
21. Limestone, micritic, silty, very light gray, separated from underlying unit by an irregular cherty layer	0.5	85.6
20. Limestone, micritic, silty, pinkish-gray in lower part and buff to light-gray in upper part, laminated	3.7	85.1
19. Limestone, micritic, light-gray; upper meter contains lenticular chert and rare spherical chert nodules	5.0	81.4
18. Limestone, micritic, silty, pink to light-gray, containing lenses and elongate nodules of chert. Upper part contains abundant black spherical chert nodules to 4 cm in diameter	2.4	76.4
17. Limestone, micritic, silty, pink to light-gray; nodular chert present in upper part	1.8	74.0
16. Limestone, micritic, light-gray; lower 20 cm is pinkish gray; upper 15 cm is a single bed of black chert	2.0	72.2
15. Limestone, micritic, silty, light-gray to pinkish-gray, massive. Planar concentrations of nodular chert present near top of unit	9.0	70.2
14. Limestone, micritic, light-gray, laminated	0.6	61.2
13. Limestone, micritic, silty, light-gray to light-purple, containing scattered spherical chert nodules to 2 cm in diameter. Thin-section sample MC-1-11	2.4	60.6
12. Limestone, micritic, silty, light-purple, recessive	1.0	58.2
11. Limestone, micritic, medium-gray, containing abundant spherical (to 5 cm in diameter) and elongate chert nodules in planar concentrations. Conodont sample MC-1-10 from middle part of unit	3.0	57.2
10. Limestone, micritic, silty, pinkish-gray to light-gray, fissile and recessive; weathers to platy fragments about 1 cm thick. Subordinate medium-gray micritic limestone in beds 5–15 cm thick	9.5	54.2
9. Limestone, micritic, light- to medium-gray, in beds 5–20 cm thick commonly separated by silty layers less than 1 cm thick	2.4	44.7
8. Limestone, micritic, gray; overlies dark-gray limestone ledge equivalent to 7	0.5	42.3
[Section repeated by faulting. Measurement resumed across fault at top of a dark-gray limestone bed equivalent to 7]		
7. Limestone, micritic, dark-gray; forms ledge. Contains buff silty lenses and beds 1–5 cm thick and scattered spherical chert nodules 1–4 cm in diameter. Locally shows contorted bedding. Conodont sample MC-1-9 from base of unit	3.4	41.8
Member 1 (units 6 and 5, total thickness 38.4 m):		
6. Covered interval	0.5	38.4

5. Limestone, micritic, silty, buff, forming resistant, planar beds 50 cm to 3 m thick. Lenses and beds of dark-brown chert 3–10 cm thick common, particularly near the tops of silty limestone beds. Resistant beds generally separated by recessive layers of buff to pinkish-gray silty limestone or calcareous siltstone 3–15 cm thick. Bases of resistant beds gradational with the underlying recessive layers; tops of resistant beds sharp. Conodont and thin-section sample MC-1-4 from 1.5 m above base of unit; conodont sample MC-1-5 from 10 m above base of unit	37.9	37.9
Thickness of Bird Spring Formation	601.3	
Indian Springs Formation (Mississippian):		
4. Covered interval	14.5	16.8
3. Limestone (calcarenite), gray. Coarse bioclasts (brachiopod shell fragments and crinoid debris to 1 cm) scattered throughout bed and concentrated in crude planar layers several centimeters thick. Conodont and thin-section sample MC-1-2	0.8	2.3
2. Shale, greenish gray, fissile, poorly exposed	1.5	1.5
Total thickness of Indian Springs Formation	16.8	
Santa Rosa Hills Limestone (Mississippian) (not measured):		
1. Limestone, medium-gray, crinoidal, massive. Conodont samples MC-l-l and 90-MC-1 from upper 1 m of unit	---	

Measured Section MC-1A

Bird Spring Formation (lower part) and Indian Springs Formation. Section is about 1 km south of Marble Canyon. Base of section is at lat 36°35'51" N., long 117° 20'26" W., elevation 2,920 ft; top of section is at lat 36°35'55" N., long 117°20'20" W., elevation 3,000 ft. Measured by Paul Stone in 1980.

	Thickness in meters	Cumulative thickness of unit in meters
Top of section		
Bird Spring Formation (Pennsylvanian) (incomplete):		
16. Limestone, dark-gray, with ochre silty bands; equivalent to 7, section MC-1; not measured	---	
15. Limestone, micritic, silty, buff, interbedded with purplish- to pinkish-gray silty limestone or calcareous siltstone; equivalent to 5, section MC-1	43.0	43.0
Incomplete thickness of Bird Spring Formation	43.0	
Indian Springs Formation (Mississippian):		
14. Siltstone, calcareous, and sandstone, very fine grained, gray to pink; some siltstone is fissile; some sandstone is weakly laminated. Contains burrows, plant fossils, abraded brachiopods, and phosphatized grains. Well exposed in one stream cut near line of measured section, but poorly exposed in most places	1.4	18.1
13. Limestone, sandy, conglomeratic, containing dark-brown phosphatic clasts to 2 cm in diameter. Thin-section sample MC-1A-6	0.3	16.7

12. Sandstone, calcareous, light-gray; weathers medium gray to rust. Fine- to medium-grained, plane-laminated and cross-laminated. Forms ledge. Thin-section sample MC-1A-4; conodont and thin-section sample MC-lA-5	2.0	16.4
11. Sandstone, calcareous, as in 10; weathers to platy outcrops	0.6	14.4
10. Sandstone, calcareous, light-red; weathers rusty brown. Fine-grained, plane-laminated and cross-laminated. Forms ledge. Thin-section samples MC-1A-3A, -3B	0.3	13.8
9. Covered interval. Float is light-gray calcareous sandstone as in 8	0.4	13.5
8. Sandstone, calcareous, similar to 7 but forms subdued outcrop ledges 15–20 cm thick. Vaguely laminated	1.0	13.1
7. Sandstone, calcareous, light-gray; weathers dark brown. Fine-grained; plane-laminated and cross-laminated. Forms prominent ledge. Thin-section sample MC-1A-2	0.9	12.1
6. Covered interval	2.5	11.2
5. Limestone, sandy, fine- to coarse-grained, plane-laminated and cross-laminated, poorly exposed	2.0	8.7
4. Covered interval. Float is greenish-gray and reddish-brown shale	4.0	6.7
3. Limestone (calcarenite), dark-gray, coarse-grained. Basal 10 cm is coquina composed of brachiopod shell fragments and crinoidal debris to 1 cm in diameter. Equivalent to 3, section MC-1	0.7	2.7
2. Covered interval. Nearby outcrops are greenish-gray and ochre shale	2.0	2.0
Total thickness of Indian Springs Formation	18.1	
Santa Rosa Hills Limestone (Mississippian) (not measured):		
1. Limestone, light-gray, crinoidal, massive. Conodont and thin-section sample MC-1A-1 from upper 1 m of unit	---	

Measured Section MC-2

Darwin Canyon Formation (incomplete), Osborne Canyon Formation, and Bird Spring Formation (upper part). Base of section is in a side canyon 1.3 km northwest of its junction with Marble Canyon at lat 36°37'00" N., long 117°21'41" W., elevation 2,960 ft; section extends eastward across a ridge (elevation 3,480 ft) and then down slope to its top at lat 36°37'12" N., long 117°21'01" W., elevation 2,800 ft. Measured by Paul Stone in 1980, with additions and modifications by Paul Stone, C.H. Stevens, and Paul Belasky in 1990.

	Thickness in meters	Cumulative thickness of unit in meters
Top of section faulted		
Darwin Canyon Formation (Permian) (incomplete):		
84. Interval largely covered. Few outcrops of brown-weathering siltstone to very fine grained sandstone	88.0	399.3
83. Limestone (calcarenite), dark-gray, fine-grained	1.5	311.3
82. Siltstone to very fine grained sandstone, as in 54. Abundant cross lamination. Poorly exposed	35.0	309.8
81. Mudstone, pink, containing scattered dark-gray limestone clasts as much as 5 cm in diameter	3.0	274.8

80. Limestone, dark-gray, fine-grained	1.5	271.8
79. Siltstone to very fine grained sandstone, as in 54	23.0	270.3
78. Limestone (calcarenite), dark-gray, coarse-grained, massive. Clasts are echinoderm debris and intraclasts. Contains irregular lenses of fine-grained, laminated siltstone. Conodont and thin-section sample MC-2A-3	2.5	247.3
77. Siltstone to very fine grained sandstone, laminated; minor thin-bedded chert	1.0	244.8
76. Limestone (calcarenite), dark-gray, fine- to medium-grained; faintly laminated. Base and top sharp	1.0	243.8
75. Siltstone to very fine grained sandstone, calcareous, and calcarenitic limestone, silty to sandy, in beds 10–40 cm thick. Alternates with recessive intervals of thin-bedded purple mudstone, pinkish-gray to buff siltstone, and dark-gray chert. Thin-section sample MC-2A-2 (chert) from upper 1 m of unit	8.0	242.8
74. Mudstone, calcareous, purplish-gray, massive. Thin-section sample MC-2A-1	1.3	234.8
73. Mudstone, pink to purple, containing spherical limestone concretions. Thin interbeds of dark-gray siliceous limestone	2.0	233.5
72. Covered interval	12.5	231.5
71. Siltstone to very fine grained sandstone, calcareous, and calcarenitic limestone, silty to sandy, as in 63. Thin-section sample MC-2-23 from 5 m above base of unit	15.0	219.0
70. Limestone (calcarenite), dark-gray, coarse-grained, massive. Forms a conspicuous marker bed. Conodont and thin-section sample MC-2-22	2.0	204.0
69. Covered interval	2.5	202.0
68. Limestone (calcarenite), dark-gray. Graded from coarse-grained, plane-laminated limestone at base to medium-grained, cross-laminated limestone at top	0.8	199.5
67. Siltstone to very fine grained sandstone, calcareous, and calcarenitic limestone, silty to sandy, as in 63. Convolute lamination common. Poorly exposed	26.3	198.7
66. Siltstone to very fine grained sandstone, calcareous, and calcarenitic limestone, silty to sandy, as in 63	13.0	172.4
65. Conglomerate, massive, containing tightly packed, spherical limestone clasts as much as 3 cm in diameter	0.5	159.4
64. Limestone (calcarenite), medium-gray, fine-grained; forms flaggy outcrops. Locally contains limestone intraclasts, as much as 3 cm in diameter, that float in the calcarenite matrix	6.4	158.9
63. Siltstone to very fine grained sandstone, calcareous, and calcarenitic limestone, silty to sandy, very fine grained; light-gray to buff; plane-laminated and cross-laminated. Individual beds not distinct. Thin-section sample MC-2-20	19.2	152.5
62. Conglomerate, massive, containing loosely packed, spherical to elongate limestone clasts embedded in a matrix of coarse-grained calcarenite	0.5	133.3

61. Limestone (calcarenite), light-gray, silty to sandy; cross-laminated	7.0	132.8
60. Limestone (calcarenite), coarse-grained, locally grading into conglomerate. Composed of coarse crinoidal debris and dark-gray, subrounded limestone clasts as much as 3 cm in diameter. Thin interbeds and lenses of buff-weathering silty limestone are common. Conodont sample MC-2-19	1.5	125.8
59. Siltstone to very fine grained sandstone, as in 54, and minor laminated, silty to sandy calcarenitic limestone	18.0	124.3
58. Siltstone to very fine grained sandstone, as in 54. Top of unit is at crest of ridge. Thin-section sample MC-2-18, 5 m above base of unit	25.0	106.3
57. Siltstone containing abundant spherical to rod- or disc-shaped limestone clasts. Clasts float in siltstone matrix	0.3	81.3
56. Siltstone to very fine grained sandstone, as in 54	13.0	81.0
55. Conglomerate, forming a single, crudely graded bed. Clasts in lower 0.3 m are of dark-brown-weathering chert, subangular, as much as 5 cm in diameter. Clasts in upper 0.7 m are of limestone, subrounded, as much as 2 cm in diameter. Uppermost 5 cm plane 1aminated. Thin-section sample MC-2-17	1.0	68.0
54. Siltstone to very fine grained sandstone, slightly calcareous. Fresh surfaces pale-red, light reddish gray, or pale-gray; weathered surfaces dark-brown. Commonly plane laminated and cross-laminated. Stands out in thick ledges that alternate with relatively recessive intervals. Individual beds not distinct. Unit contains minor silty to sandy calcarenitic limestone as in 53 and 51. Thin-section sample MC-2-16 (calcareous sandstone) from 20 m above base of unit	38.0	67.0
53. Calcarenitic limestone, silty, as in 51. One 0.3-m-thick bed of conglomerate containing spherical limestone clasts near middle of unit. Thin-section sample MC-2-15 (calcarenitic limestone) from middle part of unit	20.0	29.0
52. Chert, light-gray, massive, containing dark-gray limestone patches. Unit may be silicified limestone	1.0	9.0
51. Limestone (calcarenite), silty or sandy, light- to medium-gray; weathers buff to brown; very fine grained; finely plane laminated and cross-laminated	8.0	8.0
Incomplete thickness of Darwin Canyon Formation	399.3	
Osborne Canyon Formation (Permian):		
Member 4 (units 50–36, total thickness 23.6 m):		
50. Limestone (calcarenite), dark-gray, coarse-grained, plane-laminated. Forms ledge. Conodont sample MC-2-14	0.6	149.8
49. Mudstone, silty, calcareous, buff-weathering, thinly interbedded with gray chert	1.9	149.2
48. Limestone (calcarenite), dark-gray to light-pink, coarse-grained, bioclastic	0.3	147.3
47. Mudstone, silty, purplish-red	0.1	147.0

46. Conglomerate, containing tightly packed, spherical limestone clasts 2–4 cm in diameter	0.3	146.9
45. Interval largely covered; some outcrops of purplish-red silty mudstone	2.0	146.6
44. Mudstone, silty, calcareous, light-gray, irregularly interbedded with dark-gray, fine-grained silty limestone	1.5	144.6
43. Mudstone, silty, purplish-red, massive, containing spherical limestone concretions and ammonoids, as in 41	1.4	143.1
42. Limestone (calcarenite), dark-gray, medium- to coarse-grained; forms ledge	0.3	141.7
41. Mudstone, silty, purplish-red, massive, containing spherical limestone concretions 3–6 cm in diameter and ammonoids, some of which are in concretions	2.2	141.4
40. Mudstone, silty, calcareous, light-gray, containing dark-gray limestone concretions aligned with bedding	0.4	139.2
39. Mudstone, silty, buff to pinkish-gray; sandstone, fine-grained, laminated, in even beds 5–15 cm thick; and chert, gray, lenticular to thin-bedded (10 percent of unit). Mudstone contains sparse spherical limestone concretions. Thin-section sample MC-2-13 (chert and siltstone) from 1 m above base of unit	9.7	138.8
38. Conglomerate, containing tightly packed, well sorted, spherical limestone clasts 2–4 cm in diameter	0.2	129.1
37. Mudstone, silty, calcareous, buff, laminated, and minor thin-bedded chert. Thin-section sample MC-2-12	2.0	128.9
36. Limestone (calcarenite), dark-gray, medium- to coarse-grained, plane-laminated; and a few thin (5 cm) intervals of buff-weathering calcareous mudstone or siltstone. Conodont samp1e MC-2-11	0.7	126.9
Member 3 (units 35–14, total thickness 46.7 m):		
35. Conglomerate, containing tightly packed, spherical limestone clasts; grades upward into dark-gray, coarse-grained, laminated calcarenitic limestone	1.0	126.2
34. Covered interval	2.0	125.2
33. Conglomerate, containing tightly packed spherical and angular limestone clasts	2.5	123.2
32. Covered interval	2.0	120.7
31. Conglomerate, as in 14	0.4	118.7
30. Mudstone, silty, purple, laminated	0.9	118.3
29. Conglomerate, as in 14	1.0	117.4
28. Mudstone, silty, purple, laminated, containing sparse spherical limestone concretions or clasts	0.4	116.4
27. Conglomerate, as in 14	2.7	116.0
26. Mudstone, silty, purple, containing containing sparse spherical limestone concretions or clasts	1.2	113.3
25. Conglomerate, as in 14	0.3	112.1
24. Interval largely covered. Few outcrops of purple silty mudstone and thin-bedded chert	6.0	111.8

23. From top to bottom, consists of: conglomerate, as in 14, 0.4 m; parting plane; conglomerate, as in 14, 0.6 m; mudstone, silty, purple, containing aligned, spherical limestone concretions, 1.9 m; conglomerate, as in 14, 0.5 m.....	3.4	105.8
22. Mudstone, silty, calcareous, massive, containing spherical limestone concretions or clasts; locally laminated. Conodont and thin-section sample MC-2-10 (limestone concretions) from 2 m above base	4.0	102.4
21. Conglomerate, as in 14	2.4	98.4
20. From top to bottom, consists of: mudstone, silty, containing sparse, spherical limestone concretions, 2.3 m; conglomerate, as in 14, 0.2 m; chert and silty mudstone, 1.0 m; conglomerate, as in 14, 0.7 m; chert and silty mudstone, 0.1 m; conglomerate, as in 14, 0.6 m	4.9	96.0
19. Mudstone, silty, pink to purple, containing spherical limestone concretions (75 percent); and chert, thin-bedded (25 percent). Thin-section sample MC-2-9 (mudstone)	9.0	91.1
18. Conglomerate, as in 14	0.7	82.1
17. Silty mudstone and chert	0.1	81.4
16. Conglomerate, as in 14	0.6	81.3
15. Silty mudstone and chert	0.3	80.7
14. Conglomerate, forming a resistant ledge. Consists of poorly sorted, spherical limestone clasts 1–15 cm in diameter in a light-gray, silty limestone matrix. Rock is clast-supported (clasts make up 70 percent of rock)	0.9	80.4
Member 2 (units 13–10, total thickness 43.5 m):		
13. Chert, silty mudstone, and limestone concretions, as in 11	3.0	79.5
12. Mudstone, silty, massive, containing 60–80 percent spherical limestone concretions. Thin interbeds of chert and pink mudstone	4.0	76.5
11. Chert, black, thin-bedded (75 percent); and mudstone, pink, silty, containing spherical limestone concretions (25 percent). Some intervals, 0.2–0.8 m thick, consist almost entirely of limestone concretions	8.5	72.5
Member 1 (units 9–7, total thickness 36.0 m):		
10. Mudstone, silty, purple, and chert, black, intercalated in beds 1–4 cm thick. Mudstone contains abundant limestone concretions 2–15 cm in diameter. Concretions range in shape from spherical to somewhat flattened in the plane of bedding. Forms slope. Thin-section sample MC-2-5 (chert) from just above base of unit	28.0	64.0
9. Silty mudstone and fine-grained sandstone, as in 7 and 8; less sandstone than in 8	5.0	36.0
8. Silty mudstone and fine-grained sandstone, as in 7; sandstone beds rarely thicker than 10 cm; poorly exposed	15.0	31.0
7. Mudstone, silty, pinkish-gray, purplish-gray, greenish gray, and buff, weakly calcareous (70 percent); and sandstone, calcareous, medium-gray, fine-grained, plane-laminated and cross-laminated (30 percent). Sandstone forms discrete beds 2–20 cm thick that		

have sharp bases and tops. Rare lenses of dark-gray, micritic limestone. Thin-section samples MC-2-3A, -3B, -3C, and -3D, all from lower 3 m of unit; conodont sample MC-2-4 (limestone lens)	16.0	16.0
Total thickness of Osborne Canyon Formation	149.8	
Bird Spring Formation (Pennsylvanian) (incomplete):		
6. Limestone, micritic, silty; light-gray on fresh surfaces; weathers buff to pinkish-gray. Some plane lamination. One bed of dark-gray silty limestone, 0.4 m thick, containing abundant coarse crinoidal debris, near middle of unit	12.0	65.0
5. Interbedded pinkish-gray to purplish-gray silty limestone (20 percent) and medium-gray limestone (80 percent), both micritic. Local concentrations of coarse-grained crinoidal debris. Conodont sample MC-2-1 from upper 1 m of unit	6.0	53.0
4. Interbedded pinkish-gray to purplish-gray silty limestone (75 percent) and medium-gray limestone (25 percent), both micritic. Medium-gray layers 20-40 cm thick. Chert more abundant than in 3 but not as abundant as in 2	12.0	47.0
3. Interbedded pinkish-gray to purplish-gray silty limestone (75 percent) and medium-gray limestone (75 percent), both micritic. Chert rare	8.0	35.0
2. Limestone, micritic, silty; weathers buff to pinkish gray; contains abundant layered chert, lenticular chert, and aligned elongate chert nodules	27.0	27.0
1. Limestone (packstone), crinoidal, massive; not measured	---	
Incomplete thickness of Bird Spring Formation	65.0	

Appendix 2—Mississippian Conodonts, by C.A. Sandberg

Faunal lists indicate number of specimens of each element. See Clark and others (1981) and Sweet (1988) for definitions of element types (for example, Pa, Pb, Sc).

Stone Canyon Limestone

Measured Section CC

PD17. Unit 3, 1 m above base of Stone Canyon Limestone

Bispathodus utahensis
1 Pa element
3 M elements
2 Sc elements
2 *Gnathodus* sp.; Pa elements
1 *Hindeodus* sp.; Pa element
17 *Polygnathus communis*; Pa elements
6 *Pseudopolygnathus nudus* morphotype 1; Pa elements
5 *Pseudopolygnathus nudus* morphotype indet.; Pa elements
1 *Pseudopolygnathus oxypageus* morphotype 3; Pa element
1 *Vogelgnathus* n. sp.; Pa element

1 *Bactrognathus* n. sp.; Pb element
1 *Hindeodella segaformis*; Sc element

Age: Upper *typicus* zone (Middle Mississippian, early middle Osagean)

CC-1. Unit 5, 260 m above base of Stone Canyon Limestone

Bispathodus utahensis
29 Pa elements
3 Pb elements
28 Sc elements
2 *Doliognathus latus* morphotype 3; Pa elements
59 *Eotaphrus burlingtonensis*; Pa elements
37 *Eotaphrus* sp.; M elements
3 *Polygnathus communis*; Pa elements
1 *Bactrognathus* n. sp. LSZ; Pa element
17 *Hindeodella segaformis*; Sc elements
15 indeterminate Pb elements
2 indeterminate Sa elements

Age: *anchoralis-latus* zone (Middle Mississippian, middle Osagean)

CC-4. Unit 7, ~50 m below top of Stone Canyon Limestone

1 *Bispathodus utahensis*; Pa element
3 *Eotaphrus burlingtonensis*; Pa elements
1 *Ligonodina* sp.; Sc element

Age: *anchoralis-latus* zone (Middle Mississippian, middle Osagean)

Santa Rosa Hills Limestone

Measured Section CC

CC-6. Unit 8, 16 m above base of Santa Rosa Hills Limestone

1 *Bispathodus utahensis*; Pa element
14 *Hindeodus cristulus*; Pa elements
1 *Ligonodina* sp.; Sc element
1 *Polygnathus communis*; M element

Age: *mehli*-Lower *texanus* zone (Middle Mississippian, late Osagean)

Measured Section MC-1

MC-1-1. Unit 1, upper 1 m of Santa Rosa Hills Limestone

2 *Bispathodus stabilis*; Pa elements
8 *Hindeodus penescitulus*; Pa elements
2 *Taphrognathus varians*; Pa elements
1 *Vogelgnathus campbelli*; Pa element

1 *Magnilaterella* sp.; Sd element
3 indeterminate M elements
1 indeterminate Sa element

Age: *homopunctatus*-Upper *texanus* zone (Middle Mississippian, early Meramecian)

Measured Section MC-1A

MC-1A-1. Unit 1, upper 1 m of Santa Rosa Hills Limestone

1 *Taphrognathus varians*?; broken

Age: Middle Mississippian, Meramecian

Spot Localities

90-MC-1. Upper 1 m of Santa Rosa Hills Limestone, approximately same locality as MC-1-1 at base of measured section MC-1

Bispathodus utahensis
7 Pa elements
4 M elements
1 Sb element
2 *Hindeodus cristulus*; Pa elements
2 *Hindeodus penescitulus*; Pa elements
3 *Taphrognathus varians*; Pa elements
6 *Kladognathus* sp.; Sc elements
3 indeterminate M elements

Age: *homopunctatus*-Upper *texanus* zone (Middle Mississippian, early Meramecian)

79-CC-49. 4 m below top of Santa Rosa Hills Limestone, lat 36°36'15" N., long 117°21'48" W.

1 *Cloghergnathus? sp.*
1 *Apatognathus?*; Sa element

Age: Middle Mississippian, Meramecian

Indian Springs Formation

Measured Section MC-1

MC-1-2. Unit 3, ~2 m above base of Indian Springs Formation

23 *Gnathodus bilineatus* morphotype alpha

Age: *bilineatus*-Upper *Cavusgnathus* zone (Late Mississippian, early Chesterian)

Measured Section MC-1A

MC-1A-5. Unit 12, upper 1 m of Indian Springs Formation

3 *Gnathodus bilineatus*; fragments
3 *Rhachistognathus muricatus*; fragments
1 *Adetognathus* sp.; fragment

Age: Late Mississippian, late Chesterian

Appendix 3—Pennsylvanian and Permian Conodonts, by B.R. Wardlaw

Bird Spring Formation

Measured Section MC-1

MC-1-4. Unit 5, 1.5 m above base of Bird Spring Formation

Material: 16 platforms and fragments

Idiognathoides sinuatus
Idiognathodus sp. (juvenile)

Age: Bashkirian

Note: The lowest collections from the Bird Spring Formation at Marble Canyon contain *Idiognathoides sinuatus*, which does not make its first appearance at Arrow Canyon, Nevada, until well up in the Bird Spring Formation (*sinuatus-minutus* Zone; Lane and others, 1999). The Marble Canyon section is therefore missing strata of earliest Bashkirian age. This interpretation is consistent with the earlier interpretation of J.R. Repetski (*in* Stone, 1984), who considered samples MC-1-4 through MC-1-15 to represent an age of medial to late(?) Morrowan.

MC-1-5. Unit 5, 10 m above base of Bird Spring Formation

Material: 147 platforms and fragments heavily coated with quartz silt

Idiognathoides sinuatus

Age: Bashkirian

MC-1-9. Unit 7, ~38.5 m above base of Bird Spring Formation

Material: 77 platforms and fragments, mostly bars

Idiognathoides sp.
Idiognathodus
Hindeodus?

Age: Bashkirian

MC-1-10. Unit 11, ~55 m above base of Bird Spring Formation

Material: 28 platforms and fragments

Idiognathoides sp.
Idiognathodus sinuosis
Neognathodus
Gnathodus sp.
Idiognathodus sp.

Age: Bashkirian

MC-1-15. Unit 25, ~108 m above base of Bird Spring Formation

Material: 24 platforms and fragments

Idiognathodus sp.

Age: Bashkirian

MC-1-16. Unit 26, ~119 m above base of Bird Spring Formation

Material: 7 platforms and bars

Idiognathodus sinuosis

Age: Bashkirian

MC-1-18. Unit 34, ~132 m above base of Bird Spring Formation

Material: 34 platforms and fragments

Idiognathodus sinuosis
Idiognathoides sp.

Age: Bashkirian

MC-1-25. Unit 53, ~258 m above base of Bird Spring Formation

Material: 1 platform

Idiognathodus amplificus

Age: Moscovian

MC-1-26. Unit 54, ~265 m above base of Bird Spring Formation

Material: 72 platforms and fragments heavily coated with quartz silt

Idiognathodus amplificus
Idiognathodus obliquus
Neognathodus asymmetricus

Idiognathodus sp.
Mesogondolella donbasica

Age: Moscovian

MC-1-33. Unit 62, ~355 m above base of Bird Spring Formation

Material: 19 platforms and fragments

Neognathodus asymmetricus
Gondolella sp.
Idiognathodus delicatus

Age: Moscovian

MC-1-34. Unit 64, ~370 m above base of Bird Spring Formation

Material: 34 platforms and fragments

Neognathodus asymmetricus
Adetognathus lautus
Idiognathodus sp.

Age: Moscovian

MC-1-37. Unit 68, ~397 m above base of Bird Spring Formation

Material: 1 platform

Swadelina subexcelsus

Age: Moscovian

MC-1-40. Unit 73, ~419 m above base of Bird Spring Formation

Material: 1 platform

Adetognathus lautus

Age: Moscovian

MC-1-41. Unit 73, ~427 m above base of Bird Spring Formation

Material: 58 platforms and fragments; signs of hydrothermal alteration, some deformation (twisting and stretching of elements) and fracturing and healing

Idiognathodus delicatus
Neognathodus asymmetricus
Hindeodus minutus
Idiognathodus expansus

Age: Moscovian

MC-1-42. Unit 73, ~438 m above base of Bird Spring Formation

Material: 33 platforms and fragments

Idiognathodus expansus
Neognathodus asymmetricus
Adetognathus lautus

Age: Moscovian

MC-1-45. Unit 79, ~470 m above base of Bird Spring Formation

Material: 5 platforms and fragments

Hindeodus sp.

Age: Moscovian

MC-1-46. Unit 80, ~482 m above base of Bird Spring Formation

Material: 24 platforms and fragments

Idiognathodus expansus
Neognathodus asymmetricus
Adetognathus lautus
Diplognathodus sp.

Age: Moscovian

MC-1-49. Unit 87, ~515 m above base of Bird Spring Formation

Material: 89 platforms and fragments

Idiognathodus expansus
Neognathodus asymmetricus
Adetognathus lautus

Age: Moscovian

MC-1-51. Unit 89, ~538 m above base of Bird Spring Formation

Material: 20 platforms and fragments heavily coated with quartz silt

Idiognathodus expansus
Neognathodus asymmetricus
Adetognathus lautus

Age: Moscovian

MC-1-52. Unit 92, ~565 m above base of Bird Spring Formation

Material: 29 platforms and fragments heavily coated with quartz silt

Idiognathodus corrugatus

Age: Kasimovian

MC-1-53. Unit 94, ~588 m above base of Bird Spring Formation

Material: 13 fragments; all abraded grains, possibly reworked

Idiognathodus sp.

Age: Indeterminate

Measured Section MC-2

MC-2-1. Unit 5, ~13 m below top of Bird Spring Formation

Material: 75 platforms and fragments

Idiognathodus cherryvalensis
Adetognathus lautus
Hindeodus minutus
Swadelina subexcelsus

Age: Kasimovian

Osborne Canyon Formation

Measured Section MC-2

MC-2-4. Unit 7, ~8 m above base of Osborne Canyon Formation

Material: 5 fragments, some reworked

Neognathodus asymmetricus
Idiognathodus sp.
Mesogondolella sp.

Age: reworked Moscovian

MC-2-10. Unit 22, ~100 m above base of Osborne Canyon Formation

Material: 2 fragments

Neostreptognathodus clarki

Age: Artinskian

MC-2-11. Unit 36, ~126 m above base of Osborne Canyon Formation

Material: 30 platforms and fragments

Mesogondolella bisselli
Sweetognathus merrilli
Sweetognathus whitei
Neostreptognathodus clarki
Streptognathodus (reworked)

Age: Basal Artinskian

MC-2-14. Unit 50, ~149.5 m above base of Osborne Canyon Formation

Material: 111 platforms and fragments; mostly platforms; coated with silt

Sweetognathus whitei
Mesogondolella bisselli
Mesogondolella visibilis
Neostreptognathodus clarki
Streptognathodus pawkuskaensis (reworked)
Mesogondolella new species (also common to the Artinskian at Aktasty Hills, Kazakhstan)

Age: Artinskian

Darwin Canyon Formation

Measured Section MC-2

MC-2-19. Unit 60, ~125 m above base of Darwin Canyon Formation

Material: 19 platforms and fragments

Mesogondolella uralensis
Mesogondolella bisselli
Streptognathodus gracilis
Streptognathodus artinskiensis
Sweetognathus whitei

Age: Artinskian

MC-2-22. Unit 70, ~203 m above base of Darwin Canyon Formation

Material: 8 platforms and fragments

Mesogondolella uralensis
Sweetognathus whitei
Streptognathodus artinskiensis
Streptognathodus sp. (abraded, reworked)

Age: Artinskian

MC-2A-3. Unit 78, ~247 m above base of Darwin Canyon Formation

Material: 53 platforms and fragments

Sweetognathus guizhouensis
Mesogondolella new species (also common to the Aktasty Hills, Kazakhstan)
Neostreptognathodus clarki
Streptognathodus cf. *S. conjunctus* (reworked)
Streptognathodus artinskiensis
Neostreptognathodus pequopensis
Sweetognathus whitei
Mesogondolella laevigata
Streptognathodus elongatus (reworked)
Streptognathodus sp. (probably reworked)

Age: Late Artinskian

Appendix 4—Fusulinids and Other Foraminifers, by C.H. Stevens

Bird Spring Formation

Measured Section MC-1

S-1507. Unit 73, ~438 m above base of Bird Spring Formation

Beedeina cf. *B. cedarensis* (Ross and Sabins) (fig. 7*E*)
Beedeina clarkensis (Cassity and Langenheim) (fig. 7*H*)
Wedekindellina aff. *W. matura* Thompson (fig. 7*A*)
Climacammina sp.
Glyphostomella? sp.

Age: Middle Pennsylvanian, Desmoinesian

S-1508. Unit 80, ~482 m above base of Bird Spring Formation

Beedeina cf. *B. casperensis* (Thompson and Thomas) (fig. 7*C*)
Beedeina sp. (fig. 7*F*)
Climacammina sp.
Bradyina? sp.

Age: Middle Pennsylvanian, Desmoinesian

S-2100. Unit 80, ~482 m above base of Bird Spring Formation

Wedekindellina coloradoensis (Roth and Skinner) (fig. 7*B*)

Age: Middle Pennsylvanian, Desmoinesian

Darwin Canyon Formation

[Samples are from debris-flow deposit near top of exposed section]

80-MC-1. Lat 36°36'28" N., long 117°21'28" W.

Schwagerina wellsensis (Thompson and Hansen) (fig. 7*G*)

Age: Early Permian, middle to late Wolfcampian (late Sakmarian to early Artinskian)

80-MC-3. Lat 36°37'26" N., long 117°21'24" W.

Schwagerina modica Thompson and Hazzard
Schwagerina cf. *S. youngquisti* Thompson and Hansen (fig. 7*J*)
Schwagerina neolata Thompson (fig. 7*D*)
Pseudoschwagerina sp. (fig. 7*L*)
Stewartina convexa (Thompson) (fig. 7*M*)
Stewartina? sp.

Age: Early Permian, middle to late Wolfcampian (late Sakmarian to early Artinskian)

S-1487. Same locality as 80-MC-1, from a limestone clast in the debris-flow deposit

Schwagerina aff. *S. modica* Thompson and Hazzard (fig. 7*K*)
Schwagerina aculeata Thompson and Hazzard (fig. 7*I*)
Schwagerina aff. *S. campensis* Thompson
Schwagerina neolata? Thompson
Schubertella sp.

Age: Early Permian, middle to late Wolfcampian (late Sakmarian to early Artinskian)

Appendix 5—Corals, by C.H. Stevens

Bird Spring Formation

Measured Section MC-1

SJS 1073. Unit 84, ~493 m above base of Bird Spring Formation

Petalaxis yosti Stevens (fig. 8*D*)

Age: Middle Pennsylvanian, Desmoinesian (Stevens, 1995)

Darwin Canyon Formation

[Sample is from debris-flow deposit near top of exposed section]

SJS 1087. Same locality as fusulinid sample 80-MC-3

Protowentzelella variabilis Federowski (figs. 8A-C)

Age: Early Permian, middle to late Wolfcampian (late Sakmarian to early Artinskian)

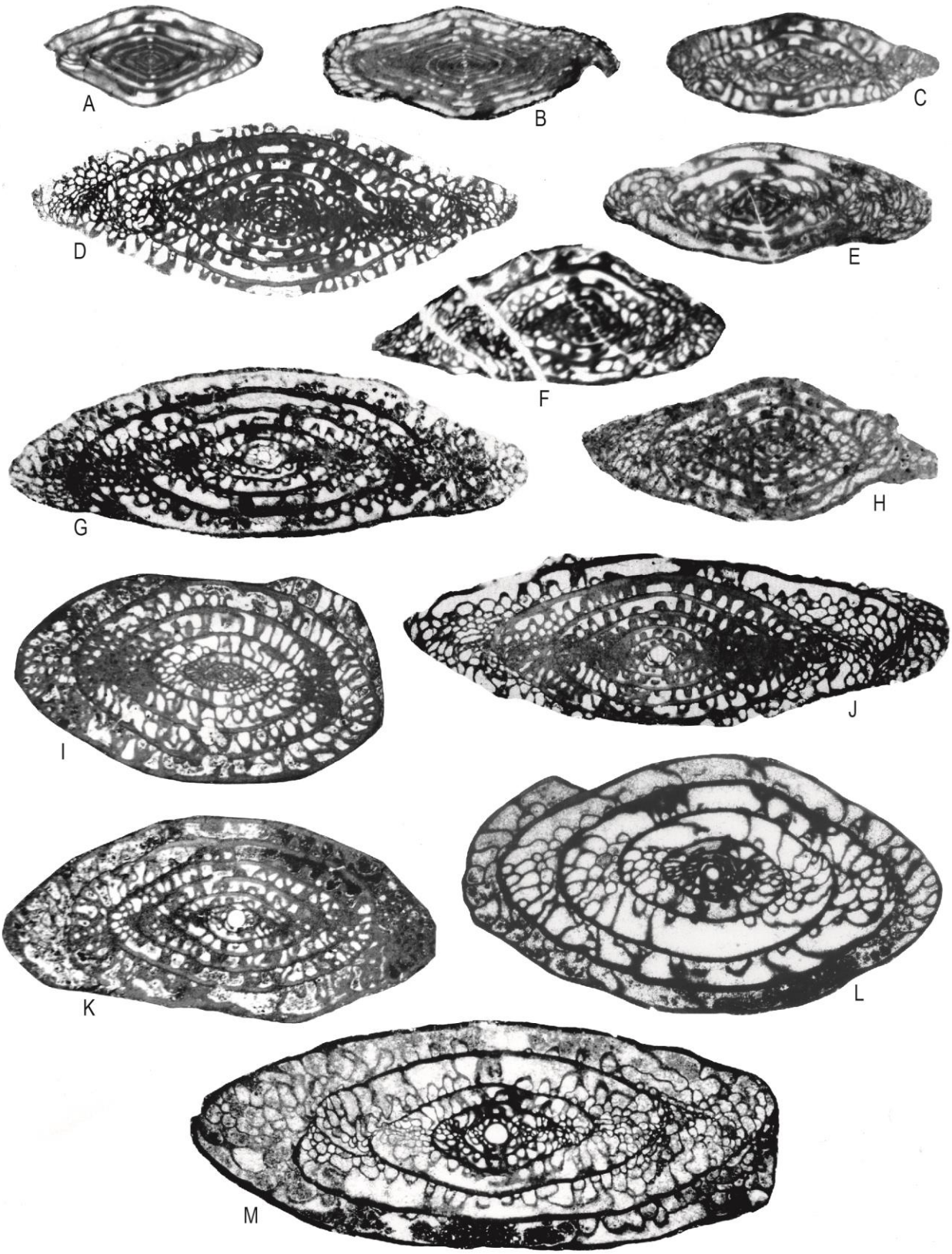
A
B
C
D
E
F
G
H
I
J
K
L
M

Figure 7. (Previous page) Thin-section photographs of fusulinids from Pennsylvanian and Permian rocks in the Marble Canyon area. All figures are axial sections. Specimens are housed in San Jose State University Museum of Paleontology, San Jose, California. *A, B, C*, *E*, *F*, *H*, fusulinids from the Pennsylvanian Bird Spring Formation, all ×15. *A*, *Wedekindellina* aff. *W. matura* Thompson, sample S-1507, slide 368f. *B*, *Wedekindellina coloradoensis* (Roth and Skinner), sample S-2100, slide 265f. *C*, *Beedeina* cf. *B. casperensis* (Thompson and Thomas), sample S-1508, slide 377f. *E*, *Beedeina* cf. *B. cedarensis* (Ross and Sabins), sample S-1507, slide 369f. *F*, *Beedeina* sp., sample S-1508, slide 371f. *H*, *Beedeina clarkensis* (Cassity and Langenheim), sample S-1507, slide 369f. *D*, *G*, *I, J, K, L, M*, fusulinids from the Permian Darwin Canyon Formation, all ×10. *D, Schwagerina neolata* Thompson, sample 80-MC-3, slide 370f. *G*, *Schwagerina wellsensis* Thompson and Hansen, sample 80-MC-1, slide 372f. *I*, *Schwagerina aculeata* Thompson and Hazzard, sample S-1487, slide 373f. *J*, *Schwagerina* cf. *S. youngquisti* Thompson and Hazzard, sample 80-MC-3, slide 374f. *K*, *Schwagerina* aff. *S. modica* Thompson and Hazzard, sample S-1487, slide 375f. *L*, *Pseudoschwagerina* sp., sample 80-MC-3, slide 376f. *M*, *Stewartina convexa* (Thompson), sample 80-MC-3, slide 378f.

Appendix 6—Thin-Section Notes, by C.H. Stevens and Paul Stone

Measured Section MC-1

Indian Springs Formation

MC-1-2. Unit 3, ~2 m above base of Indian Springs Formation

Limestone (packstone-grainstone) containing crinoid ossicles, bryozoans, fragments of brachiopod shells and spines, echinoid spines, various phosphatic fragments mostly 0.5 to 1.0 mm in diameter and 1 to 2 mm long, and small bits of phosphatized fossil fragments. Poorly sorted with calcite matrix and scattered pyrite cubes.

Bird Spring Formation

MC-1-4. Unit 5, 1.5 m above base of Bird Spring Formation

Limestone (calcisiltite), containing about 40 percent angular to subrounded quartz grains 0.05 mm in diameter; 50 percent well sorted, similar sized micritic calcite grains; minor pyrite and other opaque grains; rare muscovite.

MC-1-11. Unit 13, ~60 m above base of Bird Spring Formation

Limestone (wackestone), vaguely bedded, particles mostly 0.025 mm in diameter. Contains scattered quartz (about 25 percent), opaque minerals (probably pyrite, about 15 percent). Micrite matrix.

MC-1-14. Unit 22, ~95 m above base of Bird Spring Formation

Limestone (mudstone), relatively well bedded, containing about 10 percent siliceous sponge spicules to 0.025 mm in diameter, several ostracodes about 0.5 mm long filled with quartz, some opaque minerals (probably pyrite), and several probable calcified radiolarians up to 0.17 mm in diameter. Micrite matrix.

MC-1-17. Unit 27, ~122 m above base of Bird Spring Formation

Limestone (wackestone), very thinly bedded, containing about 10 percent siliceous sponge spicules mostly 0.025 mm in diameter, many angular quartz grains about 0.07 mm in diameter, and minor fragments of calcareous fossils. Micrite matrix.

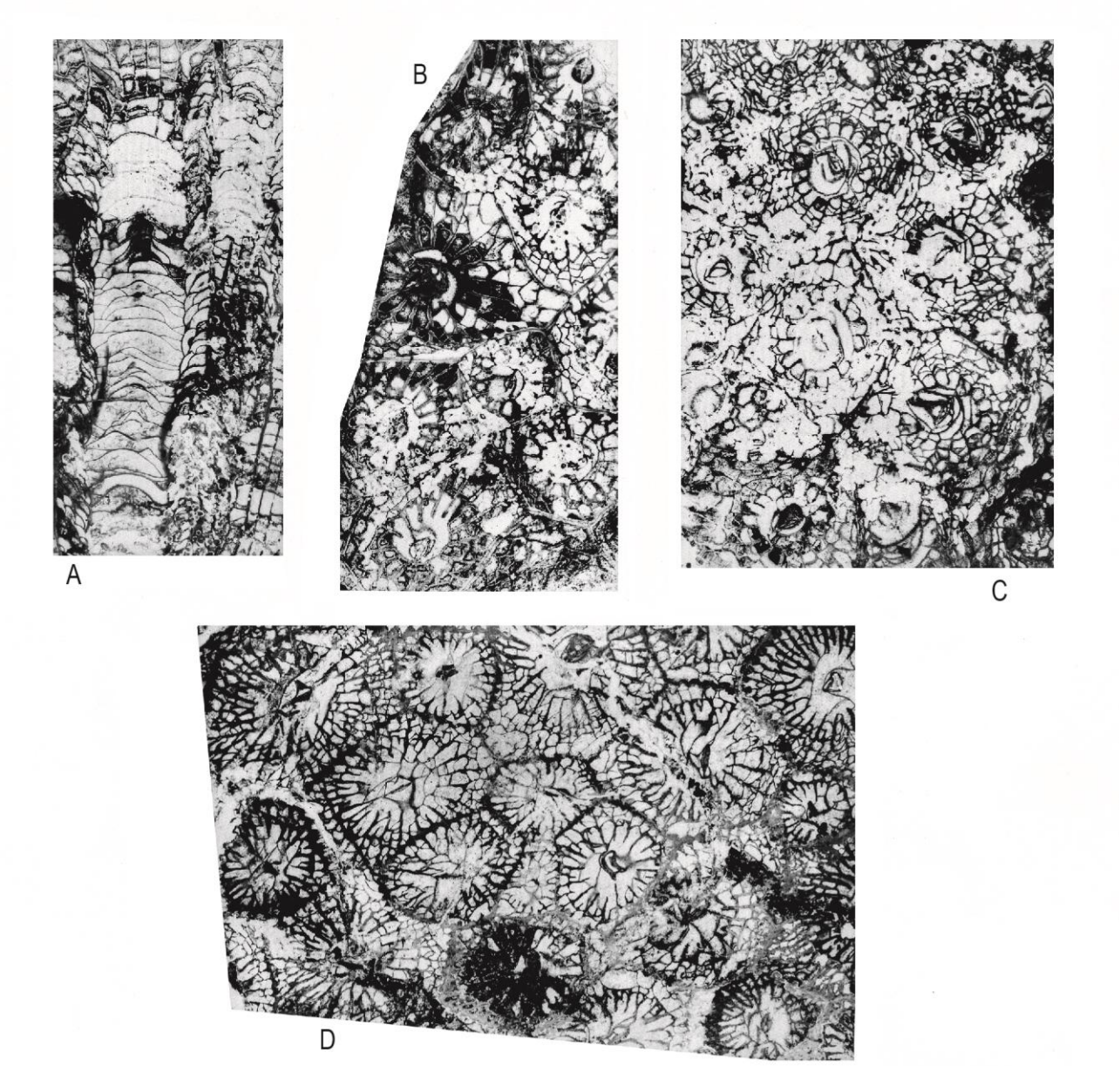

Figure 8. Thin-section photographs of colonial corals from Pennsylvanian and Permian rocks in the Marble Canyon area. *A, B, C, Protowentzelella variabilis* Fedorowski, sample SJS 1087 from the Permian Darwin Canyon Formation, all ×3. *A*, longitudinal section, slide 247c. *B*, transverse section, slide 248c. *C*, transverse section, slide 249c. *D*, *Petalaxis yosti* Stevens, sample SJS 1073 from the Pennsylvanian Bird Spring Formation, transverse section, x3.

MC-1-24. Unit 48, ~218 m above base of Bird Spring Formation

Spiculitic chert, vaguely bedded, containing 80 percent sponge spicules mostly 0.05 mm in diameter and often 0.25 to 1.0 mm long. Many spicules are replaced by calcite. Also contains less than 10 percent angular to subrounded quartz grains about 0.03 mm in diameter, a few apparent radiolarians, and some dolomite rhombs. Chert matrix.

MC-1-25. Unit 53, ~258 m above base of Bird Spring Formation

Limestone (mudstone), containing scattered pyrite and a few quartz grains to 0.05 mm in diameter. Micrite matrix.

MC-1-27. Unit 55, ~268 m above base of Bird Spring Formation

Limestone (mudstone), partially laminated, containing 60 percent unidentified fragments (some possible sponge spicules) about 0.025 mm in diameter, and pyrite. Micrite matrix.

MC-1-31. Unit 61, ~329 m above base of Bird Spring Formation

Limestone (wackestone), with disturbed bedding, containing 40 percent quartz grains 0.025 to 0.05 mm in diameter, pyrite cubes in two layers each 1 crystal thick, some dolomite rhombs, and a few sponge spicules. Matrix is part calcite and part chert.

MC-1-33. Unit 62,~355 m above base of Bird Spring Formation

Limestone (grainstone), not bedded, containing fusulinids to 1.5 mm long, crinoid columnals with overgrowths, bryozoans to 3 mm in diameter, small quartz grains, and brachiopod shell fragments to 3 mm long. Partly silicified.

MC-1-35. Unit 66, ~382 m above base of Bird Spring Formation

Limestone (mudstone) with about 10 percent quartz grains and other particles 0.025 to 0.05 mm in diameter in a micrite matrix. Half of thin section is chert with abundant small crystals of calcite or dolomite, some pyrite, and quartz grains 0.025 mm in diameter.

MC-1-41. Unit 73, ~427 m above base of Bird Spring Formation

Limestone (grainstone), containing fusulinids, crinoid columnals with overgrowths, bryozoans, *Tetrataxis*? (foraminifer), palaeotextulariid foraminifers, and echinoid spines. Fossils mostly 0.5 to 1.0 mm in diameter, rarely to 4 mm.

MC-1-48. Unit 85, ~507 m above base of Bird Spring Formation

Limestone (mudstone-packstone), vaguely bedded, containing rare sponge spicules and several larger crinoid fragments. Most particles about 0.025 mm in diameter. Matrix consists of micrite, chert, and opaque minerals.

MC-1-55. Unit 96, ~600 m above base of Bird Spring Formation

Limestone (wackestone), poorly sorted, not bedded, possibly burrowed. Contains large crinoid fragments to 2 mm in diameter, bryozoans, pellets, *Bradyina* (foraminifer), gastropods, and scattered quartz grains to 0.075 mm in diameter.

Measured Section MC-1A

Santa Rosa Hills Limestone

MC-1A-1. Unit 1, upper 1 m of formation

Limestone (grainstone), not bedded, composed entirely of crinoid fragments 1 to 2 mm in diameter and crystalline calcite.

Indian Springs Formation

MC-1A-2. Unit 7, ~12 m above base of Indian Springs Formation

Sandstone, vaguely bedded, composed of well sorted, angular to subrounded quartz grains about 0.075 mm in diameter. Minor calcite cement and opaque splotches (pyrite?).

MC-1A-3A. Unit 10, ~14 m above base of Indian Springs Formation

Sandstone, similar to MC-1A-2 but with cross lamination.

MC-1A-3B. Unit 10, approximately same locality as MC-1A-3A

Sandstone, complexly bedded, composed of angular to subrounded quartz grains 0.075 to 0.1 mm in diameter.

MC-1A-4. Unit 12, ~16 m above base of Indian Springs Formation

Sandstone, primarily composed of angular to subrounded quartz grains mostly about 1.0 mm in diameter in calcite cement. Contains various small foraminifers resembling *Millerella*, *Brunsia*, *Nodosinella* and *Agathammina*, and unidentified shell fragments.

MC-1A-5. Unit 12, approximately same locality as MC-1A-4

Sandstone, ripple-cross-bedded, composed of poorly sorted quartz grains 0.05 to 0.2 mm in diameter in calcite matrix. Contains productid spines and unidentified fossil fragments.

MC-1A-6. Unit 13, ~16.5 m above base of Indian Springs Formation

Limestone (packstone), possibly burrowed, containing abundant phosphate clasts up to 1.5 mm in diameter; rounded phosphate peloids mostly about 0.1 mm in diameter, some with accretionary structure; some small, phosphatized fossil fragments; one shell fragment 4 mm long; and a few subrounded quartz grains of various sizes up to 0.33 mm in diameter. Calcite matrix.

Measured Section MC-2

Osborne Canyon Formation

MC-2-3A. Unit 7, lower 3 m of Osborne Canyon Formation

Sandstone, crossbedded, composed of angular to subangular quartz grains 0.1 to 0.13 mm in diameter, minor pyrite, a few productid and echinoid spines, crinoids and other minor fossil debris. Micrite matrix.

MC-2-3B. Unit 7, lower 3 m of Osborne Canyon Formation

Limestone (packstone?), very thinly bedded, poorly sorted, containing 40 percent quartz grains 0.1 to 0.15 mm in diameter, a few small foraminifers, algal(?) fragments, and abundant crinoid debris up to 0.33 mm in diameter.

MC-2-3C. Unit 7, lower 3 m of Osborne Canyon Formation

Sandstone, moderately well sorted, composed of angular to subrounded quartz grains about 0.1 mm in diameter, productid spines, algal(?) fragments, and a few foraminifers, crinoid fragments, and other fossils in one layer, and scattered opaque minerals (pyrite?). Micrite matrix.

MC-2-3D. Unit 7, lower 3 m of Osborne Canyon Formation

Wackestone, unbedded, containing numerous particles including quartz 0.025 mm in diameter and minor muscovite. Micrite matrix.

MC-2-5. Unit 10, ~37 m above base of Osborne Canyon Formation

Radiolarian chert, well bedded, containing radiolarians 0.05 to 0.3 mm in diameter and several large, thin brachiopod shells in a matrix of chert and opaque minerals.

MC-2-9. Unit 19, ~86 m above base of Osborne Canyon Formation

Limestone (mudstone-wackestone), well bedded, containing abundant particles about 0.025 mm in diameter, including quartz and some possible radiolarians replaced by calcite, up to 0.15 mm in diameter.

MC-2-10. Unit 22, ~100 m above base of Osborne Canyon Formation

Limestone (wackestone), vaguely bedded, poorly preserved, mostly micrite, containing several ostracodes 1 to 2 mm across, some peloids to 0.25 mm in diameter, several chert fragments(?) about 1 mm in diameter, and possible radiolarians to 0.175 mm in diameter.

MC-2-12. Unit 37, ~128 m above base of Osborne Canyon Formation

Limestone (wackestone), well bedded, containing 30 percent quartz grains 0.05 mm in diameter, a few brachiopod spines, one ostracode, *Nodosinella*? (foraminifer), and scattered pyrite. Micrite matrix.

MC-2-13. Unit 39, ~130 m above base of Osborne Canyon Formation

Limestone (calcisiltite) and chert, well bedded, containing scattered quartz grains and other particles up to 0.05 mm in diameter.

Darwin Canyon Formation

MC-2-15. Unit 53, ~20 m above base of Darwin Canyon Formation

Limestone (calcisiltite), thinly bedded, containing 30 percent quartz grains 0.025 to 0.05 mm in diameter.

MC-2-16. Unit 54, ~40 m above base of Darwin Canyon Formation

Calcareous sandstone, thinly bedded, composed of quartz grains 0.075 to 0.1 mm in diameter in a calcite matrix.

MC-2-17. Unit 55, ~68 m above base of Darwin Canyon Formation

Conglomerate, unbedded, containing fragments of brachiopods, crinoids, bryozoans, and fusulinids, several clasts with many calcified radiolarians, and one clast with coated grains. Most clasts 2 to 3 mm long. Clasts embedded in calcareous sandstone composed of quartz grains about 0.075 mm in diameter in a calcite matrix.

MC-2-18. Unit 58, ~86 m above base of Darwin Canyon Formation

Calcareous sandstone, not bedded, composed of 50 percent angular to subrounded quartz grains 0.075 to 0.1 mm in diameter, and minor detrital plagioclase and muscovite, in a calcite matrix.

MC-2-20. Unit 63, ~142 m above base of Darwin Canyon Formation

Siltstone, well bedded, some bedding contorted. Composed of 50 percent angular to subrounded quartz grains mostly 0.05 mm in diameter, minor crinoid debris, and the foraminifers *Globivalvulina* and *Pachyphloia*. Calcite matrix.

MC-2-22. Unit 70, ~203 m above base of Darwin Canyon Formation

Limestone (grainstone?), vaguely bedded, composed of dasycladacean algae, *Tubiphytes*, fusulinids (including *Schubertella*), crinoids with overgrowths, brachiopods, bryozoans, *Girvanella*? (alga), and coated grains; all fragments about 1 to 2 mm in diameter. Fragments are embedded in sandstone composed of angular to subrounded quartz grains 0.075 mm in diameter, with calcite cement.

MC-2-23. Unit 71, ~209 m above base of Darwin Canyon Formation

Calcareous sandstone, thinly bedded, composed of 60 percent angular to subrounded quartz grains mostly 0.075 mm in diameter; also contains *Nodosinella*? (foraminifer), some larger crinoid fragments and fragments of other fossils. Calcite matrix.

MC-2A-1. Unit 74, ~234 m above base of Darwin Canyon Formation

Siltstone, composed of 70 percent quartz grains 0.05 mm in diameter, with scattered opaque minerals (pyrite?), in a calcite matrix.

MC-2A-2. Unit 75, ~242 m above base of Darwin Canyon Formation

Radiolarian chert, thinly bedded, containing radiolarians 0.05 to 0.1 mm in diameter, and some sponge spicules. Matrix composed of chert and opaque minerals.

MC-2A-3. Unit 78, ~247 m above base of Darwin Canyon Formation

Limestone (grainstone?), containing 15 percent angular to subrounded quartz grains 0.075 to 0.1 mm in diameter, *Climacammina*, *Agathammina*, and *Globivalvulina* (foraminifers), *Tubiphytes*, brachiopods, fusulinids (including *Schubertella*), crinoid fragments with overgrowths, and coated grains. Most fragments 0.75 to 1.0 mm in diameter. Calcite matrix.

Appendix 7—Tephrochronologic Analysis of Cenozoic Tuffs, by Elmira Wan and H.A. Olson

Introduction

This appendix summarizes the results of tephrochronologic analyses of volcanic glass in samples 09-MC-30 and 12-MC-168 from tuffs that are interbedded with Tertiary and Quaternary(?) sedimentary deposits (map unit QTs) in the Marble Canyon map area. Tephrochronology is a technique used to estimate the eruptive and depositional ages of a tuff, or tephra, through statistical comparison of glass composition with previously analyzed samples such as those in a large database maintained by the USGS Tephrochronology Project in Menlo Park, California. For the tuff at locality 09-MC-30, our tephrochronologic analysis is the first attempt at a correlation. For the tuff at locality 12-MC-168, our analysis was performed to compare with the original correlation and age determination of Snow and Lux (1999). Glass shards used for chemical analysis were separated from the +200 to -100 mesh size fraction (>75 to <150 micron fraction) of each sample. Glass compositions are presented in table 1.

Table 1. Chemical composition of glass from tuff samples 09-MC-30 and 12-MC-168.

[Mean normalized oxide concentrations based on electron microprobe analysis of individual glass shards for 09-MC-30 (n=19) and 12-MC-168 (n=28). Locality coordinates (referenced to NAD27) determined in the field by hand-held Global Positioning System]

Sample	Lat/Long	SiO_2	Al_2O_3	Fe_2O_3	MgO	MnO	CaO	TiO_2	Na_2O	K_2O	Total
09-MC-30	N36°35'17.6" W117°20'05.4"	78.01	13.32	0.54	0.05	0.07	0.36	0.09	2.72	4.84	100.00
12-MC-168	N36°36'43.3" W117°20'43.9"	76.60	13.17	0.72	0.02	0.08	0.47	0.07	3.05	5.83	100.01

Sample 09-MC-30

The sample locality is in a northern tributary to the main wash in Cottonwood Canyon, where the white tuff outcrop is well exposed for a distance of about 30 m in the water-washed dry stream bed (fig. 9*A*). This tuff, which is about 1 m thick, is in a sequence of conglomeratic strata dipping ~20° NE. The dip of these strata is significantly less steep than that of underlying sandstone and minor conglomerate, which dip as much as 60° NE (see geologic map). The contact between the two sequences, however, has not been mapped.

Microscopic examination shows that the whole-grain, +200 to -100 mesh size fraction of the sample is composed of ~72 percent glass shards, ~50 percent of which are lightly to heavily coated with carbonate and iron oxide minerals, and to a lesser extent, with clay. Shards are angular to subangular, predominantly blocky or chunky, and commonly exhibit ribs, bubble-walls, or bubble-wall junctions. Shards are also vesicular with well-hydrated, equant and irregular bubble-type, cylindrical and spindle-shaped vesicles. Webby shards are less common, and frothy or pitted shards are rare. Mineral grains in the sample include abundant calcite, common amounts of biotite and tectosilicates (feldspar and quartz), rare apatite, and other unidentified minerals.

Statistical analysis indicates that sample 09-MC-30 (table 1) has close geochemical matches with two groups of previously analyzed tuffs and tephra. One group includes the 2.22–2.14 Ma tuffs of Blind Spring Valley and other closely related early Pleistocene tephra layers (Sarna-Wojcicki and others, 2005) in east-central California and adjacent Nevada. The other group includes several tuffs of late middle Miocene age (≥12.02–11.1 Ma) from coastal California, east-central California, and Nevada (for example, sample 2379-14J of Stewart and others, 1999). Because of its relatively steep dip (20°), the tuff at locality 09-MC-30 is probably older than the tuff at locality 12-MC-168, which has a dip of only 8° and has been dated at ~3.28 Ma (Snow and Lux, 1999). We therefore consider the late middle Miocene correlation more probable than the early Pleistocene correlation. Given this tentative age estimate, it is possible that the tuff at locality 09-MC-30 is equivalent to the ~12.1 Ma tuff of the Entrance Narrows of Snow and Lux (1999), which is exposed about 5 km northeast of the study area in the lower part of the Navadu Formation.

Sample 12-MC-168

The sample locality is on the north side of Marble Canyon, near the base of a sequence of conglomeratic strata perched about 100 m above wash level. The white to yellowish-white tuff bed, which is 2–3 m thick (fig. 9*B*), is discontinuously exposed for a distance of ~150 m from the sample locality eastward, where the conglomeratic sequence terminates against a fault scarp (see geologic map). The tuff and the enclosing strata dip approximately 8° northeast.

Microscopic examination shows that the +200 to -100 mesh size fraction of sample 12-MC-168 is composed of moderately to heavily coated (iron oxides, clay), predominantly solid and blocky glass

shards. Many of the shards display bubble walls and (or) bubble wall junctions; some show ribs. Vesicular shards exhibit equant to elongate cylindrical and conical shaped vesicles. A few webby shards were noted. Mineral grains include tectosilicates, biotite, and rare hornblende.

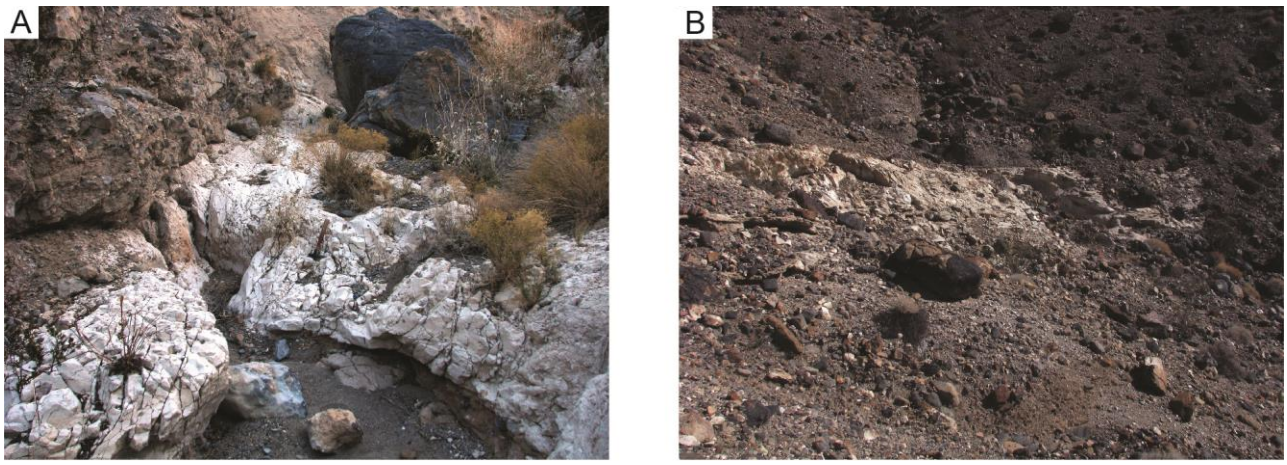

Figure 9. Photographs of Tertiary tuff outcrops in the map area. *A*, unnamed Miocene tuff at locality 09-MC-30. *B*, Pliocene tuff of Mesquite Spring near locality 12-MC-168.

Locality 12-MC-168 is essentially the same as locality 491-1 of Snow and Lux (1999), who first noted the existence of this tuff outcrop. They determined a $^{40}Ar/^{39}Ar$ age of 3.28 ± 0.15 Ma age for biotite and sanidine from the tuff, which they assigned to the Pliocene tuff of Mesquite Spring. This unit was named by Snow and White (1990) for exposures in northern Death Valley and has since been widely recognized in the Death Valley region (for example, Knott and others, 1999, 2008). Recognizing the presence of at least two separate tuffs of similar age and composition, Knott and others (1999) modified the informal unit name to tuffs of Mesquite Spring (Knott and others, 1999). Later, Knott and others (2008) referred to two of the related tuffs individually as the 3.35-Ma tuff of Zabriskie Wash and the 3.28-Ma tuff of Mesquite Spring.

Statistical analysis indicates that sample 12-MC-168 is a good geochemical match for the tuffs of Mesquite Spring, particularly the tuff of Zabriskie Wash (for example, samples JRK-DV-41, -80, -204, and -219 of Knott and others, 2008). This result is consistent with the age and correlation of this tuff originally reported by Snow and Lux (1999).

Appendix 8—Ammonoids from the Osborne Canyon Formation 5 km East of the Study Area, by Paul Stone and C.H. Stevens

In 1972, one of the authors (Stevens) collected ammonoid fossils from rocks then assigned to the lower part of the Owens Valley Formation (Johnson, 1971) near the mouth of Cottonwood Canyon, about 5 km east of the present study area. The ammonoid collections were from two closely spaced localities, 3 and 15 m above the base of the formation. Using current nomenclature, we interpret the ammonoid-bearing strata to be in the lower part of the Osborne Canyon Formation, although the precise correlation with members 1–4 at Marble Canyon is uncertain.

Ammonoid specialists W.M. Furnish and B.F. Glenister at the University of Iowa conducted a preliminary examination of the fossils and determined them to be of early Permian age (written commun., 1973). Later, the ammonoids were examined in greater detail by Lee (1975), who identified the following taxa: from the locality 3 m above the base of the Osborne Canyon Formation, *Properrinites boesei*; and from the locality 15 m above the base of the Osborne Canyon Formation,

Crimites elkoensis, *Marathonites (Almites) sellardsi*, and *Akmilleria electraensis*. According to Lee (1975), *P. boesei* is restricted to the Sakmarian, whereas the other species range through much or all of the early Permian. The photographs of ammonoid specimens originally presented by Lee (1975) are reproduced in figure 10.

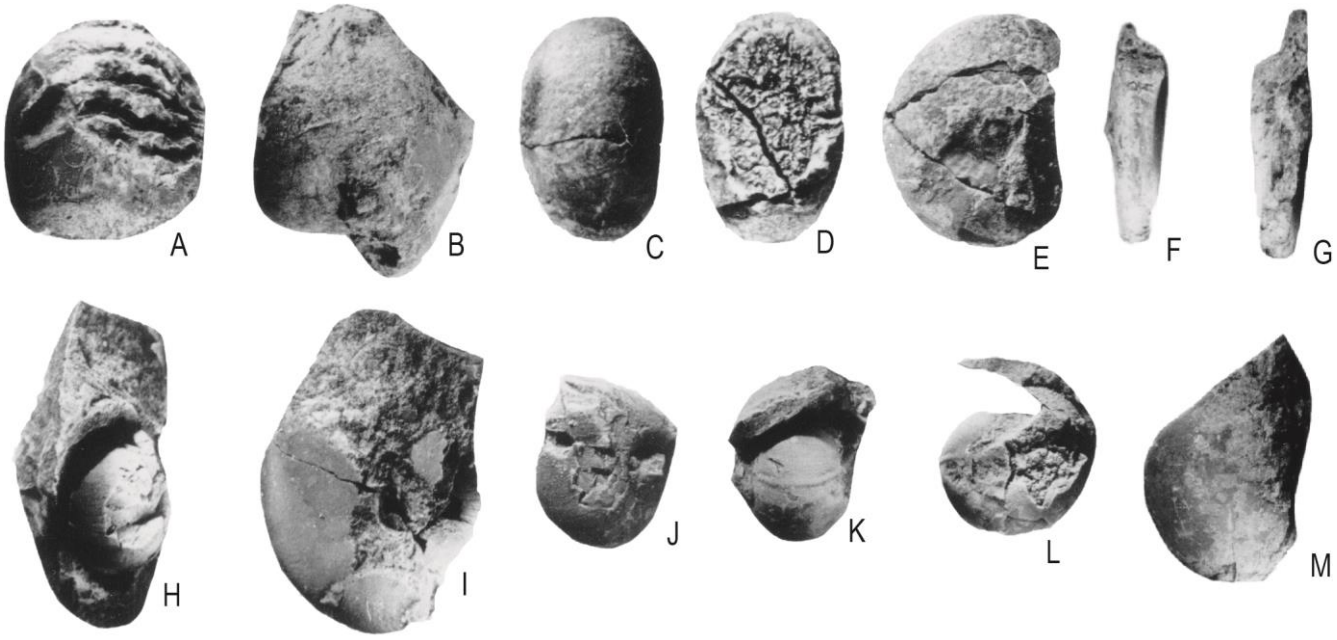

Figure 10. Photographs of ammonoids from the Osborne Canyon Formation 5 km east of the Marble Canyon study area, reproduced from Lee (1975). Specimens are housed at the University of Iowa, Iowa City. *A*, *B*, *Crimites elkoensis* Miller, Furnish, and Clark, specimen SUI 39039, ×2. *C, D, E*, *Marathonites (Almites) sellardsi* (Plummer and Scott), specimen SUI 39042, ×2. *F*, *G*, *M*, *Akmilleria electraensis* (Plummer and Scott), specimen SUI 39040, ×1. *H, I, J, K, L*, *Properrinites boesei* (Plummer and Scott); *H*, *I*, specimen SUI 39044; *J, K, L*, specimen SUI 39045; all ×2.